REDUCTION OF EDFA OPTICAL POWER TRANSIENTS USING POWER SHAPING

by

James Trent Jackson

A thesis submitted in partial fulfillment
of the requirements for the degree

of

Master of Science

in

Electrical Engineering

MONTANA STATE UNIVERSITY
Bozeman, Montana

August, 2008

APPROVAL

of a thesis submitted by

James Trent Jackson

This thesis has been read by each member of the thesis committee and has been found to be satisfactory regarding content, English usage, format, citations, bibliographic style, and consistency, and is ready for submission to the Division of Graduate Education.

Dr. Richard S. Wolff

Approved for the Department of Electrical and Computer Engineering

Dr. Robert Maher

Approved for the Division of Graduate Education

Dr. Carl Fox

STATEMENT OF PERMISSION TO USE

In presenting this thesis in partial fulfullment of the requirements for a master's degree at Montana State University, I agree that the Library shall make it available to borrowers under rules of the Library.

If I have indicated my intention to copyright this thesis by including a copyright notice page, copying is allowable only for scholarly purposes, consistent with "fair use" as prescribed in the U.S. Copyright Law. Requests for permission for extended quotation from or reproduction of this thesis in whole or in parts may be granted only by the copyright holder.

James Trent Jackson

August, 2008

ACKNOWLEDGEMENTS

I would like to thank Dr. Richard Wolff and Dr. Brendan Mumey for bringing me onto this project, for their technical advice, patience, and for helping me complete this project. Also, this work would not have been possible without the help of Dr. Wenhao Lin, Dr. Kevin Repasky, Timothy Hahn, Matt Lee, and Sriharsha Kota. A special thanks goes to my family who's support and understanding have kept me sane throughout this process.

Funding Acknowledgment

This work was kindly supported by the NSF grant number 0624874. However, any opinions, findings, conclusions, or recommendations expressed herein are those of the author(s) and do not necessarily reflect the views of the NSF.

TABLE OF CONTENTS

LIST OF FIGURES

Figure Page

LIST OF FIGURES – CONTINUED

Figure Page

LIST OF FIGURES – CONTINUED

Figure Page

ABSTRACT

Many erbium doped fiber amplifier (EDFA) based multi-wavelength optical networks employ techniques such as burst-switching or packet switching where the time interval between traffic blocks can be long enough to induce EDFA optical power transients. The optical power transients are created by abrupt changes in the average input power to the EDFAs and can adversely affect the performance of the network. To mitigate the effects of EDFA optical power transients on optical networks, a method called power shaping where heads and tails are joined to the beginning and end of a traffic block is investigated. A head (tail) gradually increases (decreases) the channel power by employing a bit sequence in which the probability of a "1" ("0") increases from 0 to 0.5. Theoretical and experimental results both show that EDFA optical power transients can be significantly reduced with adequate shaping periods. Experiments also show the bit error rate of the system is reduced for increased shaping periods. Power shaping is an economical means of suppressing EDFA optical power transients compared to other physical layer approaches that require the addition of specialized components and can be applied to EDFAs as well as other solid-state and Raman optical amplifiers.

1

INTRODUCTION

Erbium-doped fiber amplifiers (EDFAs) are an enabling technology for the development and deployment of multi-wavelength optical networks. EDFAs offer wide bandwidth that can provide gain to a large number of optical channels to offset loss due to fiber attenuation, optical losses associated with various network components, and power splitting. However, many optical networks use techniques such as burst switching and packet switching where the time interval between transmissions can be long enough to cause significant changes in the input optical power to the EDFAs. The large changes in the input optical power to EDFAs can produce optical power transients at the output of the EDFAs that can adversely affect the performance of the optical network. In the case of wavelength division multiplexed (WDM) networks, multiple optical channels can be added or dropped causing large changes to the optical power input to the EDFAs inducing cross-gain saturation and producing large optical power transients at the output of the EDFA in the surviving channels. This effect has been shown both experimentally and analytically [1, 2, 3, 4, 5, 6, 7]. It has also been reported that the magnitudes of the induced transients increase with the number of amplifiers in a chain due to the temporal characteristics of excited state lifetimes, depletion and saturation. Depending on system parameters, the power excursions in the surviving channels can be several dB causing bit errors due to nonlinear fiber optic effects if the output power is too high or an inadequate eye opening at the receiver if the output power is too low. A need exists to control the optical power transients associated with EDFAs to improve the overall network performance.

Several approaches have been proposed to mitigate EDFA transients, such as the use of optical [8, 9] or electrical [10] feedback to automatically control EDFA gain.

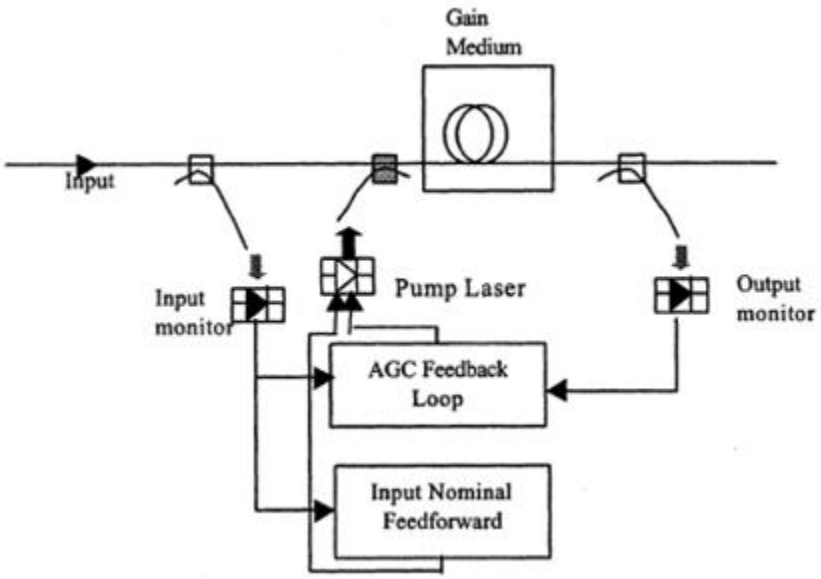

Figure 1: Illustration of a technique to reduce EDFA transients using electrical feedback [10]

A scheme that combines the use of electrical feedback and feedforward is shown in figure 1. In [10], a combination of electrical feedforward and feedback is used to control the pump laser by monitoring the input and output powers of the EDFA. The signals from the monitor outputs control the power of the pump laser which stabilizes the gain of the signal channels.

The use of optical feedback is illustrated by [9] in figure 2. The optical feedback loop is created with the use of wavelength selective optical couplers so lasing at a wavelength outside the communications band occurs. The intensity at the lasing wavelength and the intensity of channels in the communications band are inversely related. If the intensity in the communications band suddenly decreases (as in a channel drop), the lasing intensity increases and utilizes the surplus gain so that the surviving channels in the communications band see reduced transients.

Another approach is to use dummy optical signals to maintain constant input optical power as in [11, 12]. The technique for the use of dummy optical signals is

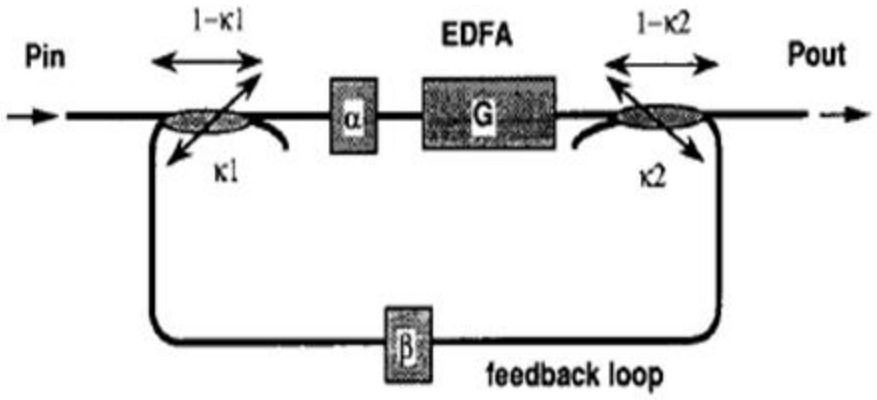

Figure 2: Illustration of optical feedback technique to reduce optical transients in EDFAs [9]

illustrated in figure 3. The dummy optical signal is created after a portion of the input optical power is converted to an electrical signal and sent to an envelope detector. The envelope detector signal is then inverted and sent to a laser whose wavelength lies outside the communications band. The signal from this out-of-band laser is mixed with the original signal so that the input power to the EDFA is constant. After passing through the EDFA, the signal from the out of band laser is filtered from the original input signals.

While these approaches have proven effective in some cases, they can be limited by slow response time [8], the use of high-power lasers [12] or by the addition of electronic [10, 11] and electro-optic components [11]. In the case of the automatic optical gain-clamped EDFA (AOGC EDFA), significant transients still occur when channels are switched on/off [13]. It has been observed that the switching time of the channel add/drop affects the EDFA transient [14] and that gradually changing the input power of the EDFA will decrease the amplitude and duration of the transients [15].

Other methods used to control EDFA optical power transients involve keeping a constant average input optical power to each EDFA in the optical network. This

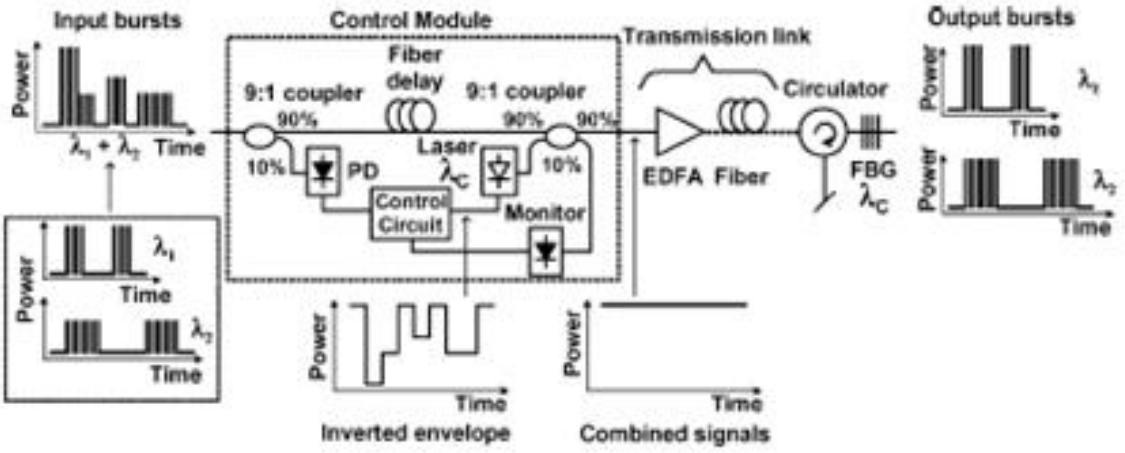

Figure 3: Illustration of the use of dummy optical signals to control optical power transients [11].

can be achieved in optical networks such as synchronous digital hierarchy (SDH) and synchronous optical networks (SONET), that employ electrical multiplexing where a continuous bit stream is transmitted along the optical link. When no user data is present, idle codes are transmitted which keeps the average power of the optical channel almost constant. Therefore, EDFA optical power transients are not a significant issue for this type of network. However, the trend is to replace these networks with all-optical systems that support optical burst switching (OBS), optical packet switching (OPS), and optical circuit switching. These types of networks operate in such a way that there can be large time intervals where the average power in a given channel is zero. The combination of dynamic channel power and long chains of EDFAs can cause significant transients to occur.

The power shaping method proposed by Wenhao Lin et. al. [15] is based on the fact that the amplitude and duration of the optical power transient generated by the EDFA is affected by how rapidly the input optical power to the EDFA changes. If the switching time for the input optical power is increased, the amplitude and duration of the optical power transient generated by the EDFA is reduced. Using this idea, a

power shaping technique has been developed for reducing the optical power transients associated with EDFAs by adding heads (tails) at the beginning (end) of a packet. A head (tail) gradually increases (decreases) the channel power by using a pseudo-random bit sequence where the probability of a "1" ("0") increases for 0 to 0.5 thus increasing the switching time of the input optical power to the EDFA. The increased switching time for the optical power reduces the amplitude and duration of the optical power transients associated with the EDFA without adding any optical or electrical components to the optical network while allowing for optical burst switching, optical packet switching, and optical circuit switching.

The key contribution of this work is experimental verification of modeling and simulations by [15] and examination of the use of different shaping profiles. This thesis is organized as follows. Chapter 2 provides a discussion of power shaping implementation considerations. The theory of the EDFA operation is presented in chapter 3. A description of the experimental setup used to study the effects of power shaping on the optical power transients generated by EDFAs is discussed in chapter 4. Power shaping is characterized in terms of the system bit error rate in chapter 5. Finally, in chapter 6, concluding remarks are presented.

6

POWER SHAPING IMPLEMENTATION

Power shaping as it applies to the reduction of EDFA optical power transients is defined as adjusting and maintaining the temporal behavior of the power of a channel or connection [15]. Power shaping techniques provide a method of gradually increasing or decreasing the average optical power input into the EDFA thus mitigating the optical power transients associated with the EDFA that adversely affect network performance. In networks where there are long idle times between continuous data frames, transients are induced on surviving channels due to the abrupt change in the input optical power to the EDFAs. By adding a head and tail to these traffic bursts, EDFA transients can be significantly reduced. A head would be a sequence of bits where the probability of a "1" is gradually increased from 0 to 0.5 while a tail is a sequence of bits where the probability of a "1" is decreased from 0.5 to 0. Heads and tails are placed at the beginning and end of the traffic block as shown in figure 4. The shape and duration of the head and tail are important and experiments to establish the effects of these parameters on transient mitigation are discussed in chapter 4.

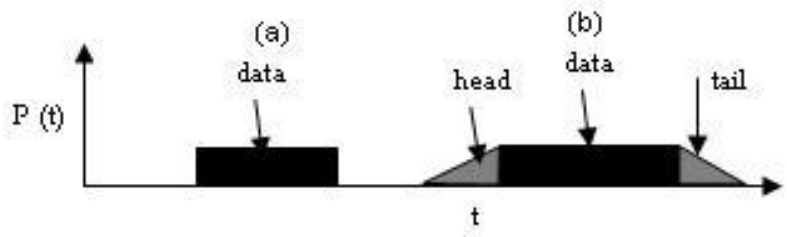

Figure 4: Illustration of the power shaping principle [15,25]

Figure 4a illustrates what the average power versus time for a channel might look like without power shaping. Transients would be created at the sharp transitions of the traffic blocks. Figure 4b illustrates the power shaping technique as it would be applied to a burst-switched network. In this case, a head is inserted at the beginning

of the first traffic block and a tail is placed at the end of the last traffic block. The application of power shaping in this case might be used in situations where the duration of the burst is much larger than the length of the heads and tail for efficiency purposes. The duration of the heads and tails is determined by the response time of the system. The response time of the system can vary greatly depending on amplifier parameters. If the time between subsequent data bursts is shorter than the response of the system, then there would be no need for heads and tails.

EDFA THEORY AND MODELING

Erbium as an Amplifier Material

Erbium doped fiber amplifiers (EDFAs) have been the enabling technology behind cost effective, long distance, multi-channel optical networks. There are several other in-line optical amplifier technologies available, and these technologies may have advantages over the EDFA in some situations. However, the EDFA remains the most popular amplifier technology for several reasons. The Er^{3+} ion has reasonably sharp fluorescence bands such that sufficient radiant power at a specific wavelength is achievable [16]. Some of these fluorescence bands occur at wavelengths corresponding to regions of low attenuation in optical fiber as shown in figure 5. Also, EDFAs have low pump thresholds, low insertion loss, polarization insensitivity, and a large signal bandwidth [3].

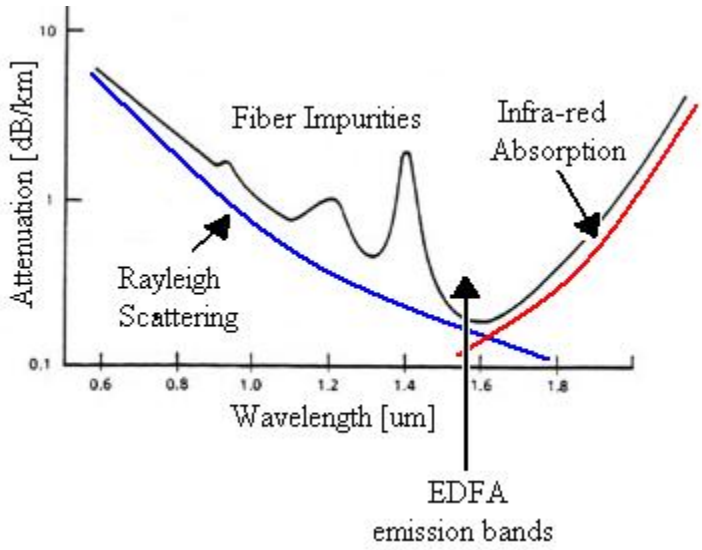

Figure 5: Attenuation in fiber versus the wavelength of light. The blue line represents Rayleigh scattering which is shown to decrease until it intersects the red line which corresponds to infra-red absorption. The humps in the black attenuation curve are due to impurities in the fiber.

In Er^{3+}, as with many other rare earth elements, exciting the atoms is made easier due to broad band pumping levels. Broad pumping levels simplify the design of pumping sources and allow the atoms to be excited with a range of photon energies. After atoms are pumped into the upper broad bands, rapid non-radiative transitions from the pumping bands into the sharp fluorescence bands occur. These fluorescence bands can have relatively long lifetimes thus allowing for population inversion and amplification to occur. In some cases, these upper fluorescence levels radiate into a level that lies above the ground state. This type of system is called a four level system. Er^{3+} is represented by a three level system where the upper fluorescence level radiates directly into the ground state as in figure 6.

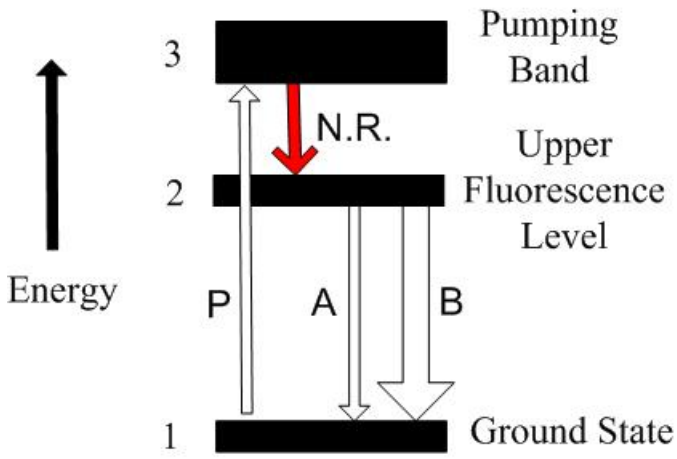

Figure 6: Illustration of the three level system. Incoming pump energy P moves population into level 3 where it rapidly relaxes into level 2 via a non-radiative process. A and B represent spontaneous and stimulated emission respectively. N.R. refers to a non-radiative process.

The three level system for Er^{3+} is an adequate representation of an EDFA operating at 1.5 μm. Rate equations for the three level system are derived and a discussion of signal gain and saturation is presented. Also, the three level model for Er^{3+} can be simplified into a two level system by making several assumptions. The two level system allows for much simpler analytical solutions to the time dependent

rate equations and numerical solutions to the time dependent rate equations are used to explain the behavior of EDFAs in the event of abrupt changes in optical power.

Analysis of a Three Level System

To derive the rate equations for the three level representation of Er^{3+} doped glass, we must first take a closer look at the three level energy diagram. Consider the three level diagram shown in figure 7 where the pumping band is represented by level 3, the fluorescence band is depicted as level 2 and level 1 is the ground state. To amplify

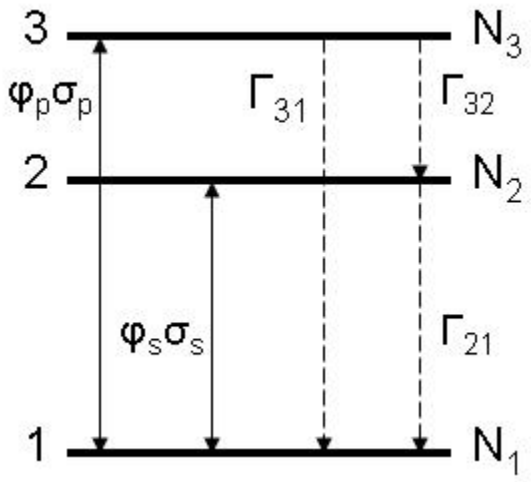

Figure 7: An illustration of the three level energy diagram where the transitions between levels 1 and 3 are proportional to the product of the cross section at the pump wavelength σ_p and the amount of pump flux φ_p. The same is true for transitions between states 1 and 2 where population in those levels is proportional to the product of the signal wavelength σ_s and the signal flux φ_s. Γ_{32}, Γ_{31} and Γ_{21} represent the spontaneous radiative and non-radiative transition rates from these levels. N_1, N_2 and N_3 are the number of ions in each state [17].

an incoming signal, population inversion must be achieved between states 1 and 2. Since Er^{3+} is a three level system, at least 50 percent of the total population must be excited from the ground state to achieve inversion. In a four level system, if level

2 (the next highest energy level from ground state) is sufficiently far away from the ground state so that thermal excitation does not occur, then any atoms that are excited from ground level form inverted populations [16]. This means that threshold pump power needed to reach population inversion is higher for a three level system. This is a significant drawback of the three level system as opposed to the four level system, but since the light in an EDFA is confined to the small core of a fiber, high intensities can be reached and population inversion is still easily achievable.

The photon flux from the pump source causes excitation of ions from level 1 to level 3 and is indicated by φ_p, and any photon flux at the signal frequency corresponding to level 2 of the diagram is denoted by φ_s. The absorption cross section for the 1 to 3 transition and the emission cross section for the 2 to 1 transition are shown as σ_p and σ_s respectively. The product of the photon flux and the cross section for a given transition is called the stimulated transition probability and will be referred to as W_{ij}. For the purposes of this analysis $W_{ij} = W_{ji}$ which assumes non-degenerate levels.

The probabilities for population to transition out of level 3 are denoted as Γ_{32} and Γ_{31}. Γ_{21} indicates the transition probability from levels 2 to 1. Γ_{32} represents the sum of radiative and non-radiative decay from level 3 to level 2 and in this case is assumed to be non-radiative. Γ_{21} for Er^{3+} is mostly composed of radiative transitions because the band gap is large enough to produce photons. This is due to the fact that there are no intermediate energy levels between level 2 and the ground state at level 1. The inverses of Γ_{32}, Γ_{31} and Γ_{21} are defined as τ_{32}, τ_{31} and τ_{21} which are called the lifetimes for the given state.

Rate Equations

Following [16, 17], the rate equations to describe the populations for the three level system are written as

$$\begin{aligned} \frac{dN_3}{dt} &= W_{13}N_1 - W_{31}N_3 - \Gamma_{32}N_3 - \Gamma_{31}N_3 \\ &= W_{13}N_1 - \alpha N_3 \end{aligned} \tag{1}$$

where $\alpha = W_{31} + \Gamma_{32} + \Gamma_{31}$. The rate equation for level 2 is given by

$$\begin{aligned} \frac{dN_2}{dt} &= W_{12}N_1 - W_{21}N_2 - \Gamma_{21}N_2 + \Gamma_{32}N_3 \\ &= W_{12}N_1 - \beta N_2 + \Gamma_{32}N_3 \end{aligned} \tag{2}$$

where $\beta = W_{21} + \Gamma_{21}$. If the total population is N, then

$$N = N_1 + N_2 + N_3 \tag{3}$$

If the system is in steady state all of the derivitives are zero

$$\frac{dN_1}{dt} = \frac{dN_2}{dt} = \frac{dN_3}{dt} = 0 \tag{4}$$

By substituting equation 3 into equation 1, N_2 can be given in terms of N_1 and the total population N

$$\begin{aligned} 0 &= W_{13}N_1 - \alpha(N - N_1 - N_2) \\ N_2 &= -N_1\left(1 + \frac{W_{13}}{\alpha}\right) + N \end{aligned} \tag{5}$$

Substituting this result into equation 2 gives the solution for the population of level N_1 in steady state

$$N_1 = \frac{\alpha\beta}{\beta\left(W_{13} + \alpha\right) + \alpha W_{12} + \Gamma_{32}W_{13}}N \tag{6}$$

Substitution of equation 6 into equation 5 gives the solution for the population of level N_2 in steady state

$$N_2 = \frac{\alpha W_{12} + \Gamma_{32}W_{13}}{\beta\left(W_{13} + \alpha\right) + \Gamma_{32}W_{13}}N \tag{7}$$

The populaion inversion per unit volume between levels 1 and 2 is then

$$\begin{aligned}\frac{\Delta N}{V} &= N_2 - N_1 \\ &= \frac{\alpha W_{12} + \Gamma_{32} W_{13} - \alpha\beta}{\beta\left(W_{13} + \alpha\right) + \alpha W_{12} + \Gamma_{32} W_{13}} N \\ &= \frac{W_{13}\left(\epsilon\Gamma_3 - \Gamma_{21}\right) - \Gamma_{21}\Gamma_3}{W_{13} + \Gamma_3\left(2W_{21} + \Gamma_{21}\right) + W_{13}\left(W_{21} + \epsilon\Gamma_3 + \Gamma_{21}\right)} N \end{aligned} \tag{8}$$

where $\Gamma_3 = \Gamma_{31} + \Gamma_{32}$ and $\epsilon = \Gamma_{32}/\left(\Gamma_{32} + \Gamma_{31}\right)$ which is the fraction of atoms that decay from the pumping absorption band into the metastable fluorescence band at level 2.

Population Inversion

In order for an EDFA to provide gain to incoming signals, population inversion between the ground state and level 2 must occur. In the case of Er^{3+}, the probability of spontaneous transitions out of level 3 is several orders of magnitude larger than the probability of transitions out of the metastable level 2 [16]. For this reason it is assumed that $\Gamma_3 >> \Gamma_{21}$. Also, for the three level model of Er^{3+}, the probability of a nonradiative decay from level 3 to level 2 exceeds that of any other level 3 process. For this reason, the population of level 3 is smaller than the other levels at any given time and the probability of creating a stimulated transition from level 3 to level 1 is much smaller than the probability of non-radiative decay from level 3 to level 2 so that $\Gamma_{32} >> W_{31}$. This approximation allows the population inversion given in equation 8 to be simplified as

$$\frac{\Delta N}{V} = N_2 - N_1 = \frac{\epsilon W_{13} - \Gamma_{21}}{\Gamma_{21} + \epsilon W_{13} + 2W_{21}} N \tag{9}$$

From the previously mentioned assumption that the probability of nonradiative decay from level 3 to level 2 far exceeds any other process of level 3, it can then be assumed

that $\Gamma_{31} \approx 0$ so that $\epsilon \approx 1$. Also, with $W_{13} = \varphi_p \sigma_p$ and $W_{21} = \varphi_s \sigma_s$ the population inversion can be written as

$$N_2 - N_1 = \frac{\varphi_p \sigma_p - \Gamma_{21}}{\Gamma_{21} + 2\varphi_s \sigma_s + \varphi_p \sigma_p} N \tag{10}$$

Assuming no background loss, population inversion occurs when $N_2 \geq N_1$. At the threshold of population inversion, $N_2 = N_1$ and the required photon flux from the pumping source is given as

$$\varphi_p = \frac{\Gamma_{21}}{\sigma_p} = \frac{1}{\tau_{21} \sigma_p} \tag{11}$$

Below threshold, N_1 is greater than N_2 and the population inversion is negative. The population inversion is positive above threshold. If the population inversion is negative, a signal passing through the media will be attenuated and if population inversion is positive, the signal will experience gain. The pump intensity in units of energy per unit area per unit time can be calculated by multiplying the pump flux φ_p by the energy of a photon at the pump frequency $h\nu_p$, where h is Plank's constant and ν_p is the frequency of a pump photon, so that $I_p = h\nu_p \varphi_p$. At the threshold of population inversion, the pump intensity is given by

$$I_{th} = \frac{h\nu_p \Gamma_{21}}{\sigma_p} = \frac{h\nu_p}{\sigma_p \tau_{21}} \tag{12}$$

Equation 12 shows that for a given pump signal frequency, the threshold intensity can be lowered by either utilizing a transition with a large cross section σ_p or by using a material with a long level 2 lifetime τ_{21}. Increasing the absorption cross section σ_p means that less pump photons are needed to excite the material because there is a greater probability that an incoming pump photon will be absorbed. A long excited state lifetime τ_{21} also reduces the number of required photons to reach threshold because more population will stay at level two for a given time. One of the reasons Er^{3+} doped glass is a good amplifier material is because the lifetime of level 2, τ_{21}, is

very long compared to many other possible materials. For Er^{3+} doped silica fiber, τ_{21} is on the order of 10 ms [17] which leads to long response time ti transients and the ringing effect seen in multiple amplifier cascades. The high value for τ_{21} also results in low pump threshold power to achieve amplification. The low threshold power is easily achieved with low cost laser diodes.

Signal Gain

To describe the gain of a signal field I_s and a pump field I_p we start with the photon fluxes which are given as

$$\varphi_s = \frac{I_s}{h\nu_s} \tag{13}$$

$$\varphi_p = \frac{I_p}{h\nu_p} \tag{14}$$

For the purpose of this analysis, the calculation of signal gain along the length of the fiber will be treated as a one dimensional problem which excludes the distribution of Er^{3+} ions in the transverse direction in the fiber core. Also, it is assumed that the pump and signal fields are copropagating beams travelling in the same direction. Equations for the derivitive of the intensity with respect to the fiber length component dz for the source and pump signals can be written as [17]

$$\frac{dI_s}{dz} = \frac{\frac{\sigma_p I_p}{h\nu_p} - \Gamma_{21}}{\Gamma_{21} + 2\frac{\sigma_s I_s}{h\nu_s} + \frac{\sigma_p I_p}{h\nu p}} \sigma_s I_s N \tag{15}$$

for the signal intensity and

$$\frac{dI_p}{dz} = -\frac{\frac{\sigma_s I_s}{h\nu_s} + \Gamma_{21}}{\Gamma_{21} + 2\frac{\sigma_s I_s}{h\nu_s} + \frac{\sigma_p I_p}{h\nu p}} \sigma_p I_p N \tag{16}$$

for the pump intensity. Setting the derivitive of the signal intensity in equation 15 to zero and solving for I_p gives

$$I_p = \frac{h\nu_p}{\sigma_p \tau_{21}} = I_{th} \tag{17}$$

which confirms the previous statement that population inversion is needed for signal gain. To simplify equations 15 and 16, the pump and signal intensities can be normalized by the threshold intensity I_{th} to give

$$I'_p = \frac{I_p}{I_{th}} \tag{18}$$

$$I'_s = \frac{I_s}{I_{th}} \tag{19}$$

Also, a new quantity η can be defined as

$$\eta = \frac{h\nu_p\sigma_s}{h\nu_s\sigma_p} \tag{20}$$

The saturation intensity is then

$$I_{sat}(z) = \frac{1 + I'_p(z)}{2\eta} \tag{21}$$

With these new quantities the normalized signal intensity as a function of z is

$$\frac{dI'_s(z)}{dz} = \frac{1}{1 + I'_s(z)/I_{sat}(z)} \left(\frac{I'_p(z) - 1}{I'_p(z) + 1} \right) \sigma_s I'_s(z) N \tag{22}$$

and the normalized pump intensity is

$$\frac{dI'_p(z)}{dz} = -\frac{1 + \eta I'_s(z)}{1 + 2\eta I'_s(z) + I'_p(z)} \sigma_p I'_p(z) N \tag{23}$$

As the signal intensity grows, it eventually enters the saturation region of the amplifier. The signal growth is damped by the $1/(1 + I'_s/I_{sat})$ term in equation 22. In the event of saturation, I'_s is large compared to I_{sat} and the ratio between the two becomes large compared to unity so that equation 22 can be approximated by

$$\frac{dI'_s}{dz} = I_{sat} \left(\frac{I'_p(z) - 1}{I'_p(z) + 1} \right) \sigma_s N \tag{24}$$

In practice and in the experiments described in chapter 4, EDFAs are operated in the saturation region. This is done to prevent small, slow changes in the power of a given input signal from changing the ouput power of that signal.

Approximation of the Three Level System by a Two Level System

Until now in the analysis, each level in the Er^{3+} energy level diagram has been treated as a single, distinct level. In reality, each energy level is a multiplet composed of several Stark broadend individual levels. If an EDFA is pumped by a 980 nm source then the pumping level lies in a different multiplet than the signal multiplet at level 2. However, it can be assumed that the population in level 3 at any given time is essentially zero due to the fact the lifetime of level 3 is several orders of magnitude shorter than the lifetime of level 2. Level 3 in this case is only involved in the rate equations by means of its absorption cross section. If a 1480 nm pumping source is used then the pump level belongs to the same multiplet as the signal level. Since the pumping level is in the same multiplet as the signal level, there will be some population in level 3 due to thermal equilibrium. In this case, the system can be reduced to a two level system using the specific absorption and emission cross sections for each level. For a pump signal whose energy level is seperate from the signal level (980 nm pump for example), the emission cross section from this level is assumed to be zero and this accounts for the fact that the population in that level is effectively zero.

Two Level Rate Equations

The rate equations for the simplfied two level system are given as

$$\frac{dN_2}{dt} = -\Gamma_{21}N_2 + (N_1\sigma_s^{(a)} - N_2\sigma_s^{(e)})\varphi_s - (N_2\sigma_p^{(e)} - N_1\sigma_p^{(a)})\varphi_p \quad (25)$$

$$\frac{dN_1}{dt} = \Gamma_{21}N_2 + (N_2\sigma_s^{(e)} - N_1\sigma_s^{(a)})\varphi_s - (N_1\sigma_p^{(a)} - N_2\sigma_p^{(e)})\varphi_p \quad (26)$$

where $\sigma_s^{(a)}, \sigma_s^{(e)}, \sigma_p^{(a)}$, and $\sigma_p^{(e)}$ represent the signal and pump absorption and emission cross sections [18]. The total population is now described as

$$N = N_1 + N_2 \tag{27}$$

and from equations 25 and 26

$$\frac{dN_1}{dt} = -\frac{dN_2}{dt} \tag{28}$$

Now after calculating the population of N_2 in terms of the signal and pump intensities, N_1 is simply given by $N - N_2$. The intensities of the pump and signal fields will experience gain or attenuation along the direction of propagation in the fiber z. This is due to the effects of absorption by ions in the ground state at level 1 and emission by ions in the excited state at level 2. The propagation equations of the signal and pump intensities are therefore described by

$$\frac{dI_p(z)}{dz} = \left(N_2\sigma_p^{(e)} - N_1\sigma_p^{(a)}\right) I_p(z) \tag{29}$$

$$\frac{dI_s(z)}{dz} = \left(N_2\sigma_s^{(e)} - N_1\sigma_s^{(a)}\right) I_s(z) \tag{30}$$

Time Dependent Analytical Solutions to the Two Level System

To characterize the behavior of an EDFA in the presence of channel addition or dropping, a simple model for the dynamic gain has been studied by [19]. The model presented by [19] shows that the EDFA can be adequately described by a single ordinary differential equation which is a simplification of previous models that use sets of coupled partial differential equations [20, 21]. To make the simplification it is assumed that there is no excited state absorption, the gain spectrum is homogeneously broadened, and the amplified spontaneous emission (ASE) power in the fiber is neglected. These assumptions are valid for signal gains less than 20 dB or when

high input powers are used such as channels in a WDM system [22]. The model starts with photon equations provided by [22, 23].

$$\frac{\partial N_k(z,t)}{\partial z} = -\frac{N_2(z,t)}{\tau} - \frac{1}{\rho S}\sum_{j=1}^{N} u_j \frac{\partial P_j(z,t)}{\partial z} \tag{31}$$

where the WDM system consists of multiple wavelengths (channels) designated by the index k. The power of the kth channel is

$$\frac{\partial P_k(z,t)}{\partial z} = \rho u_k \Gamma_k \left[\left(\sigma_k^{(e)} + \sigma_k^{(a)}\right) N_2(z,t) - \sigma_k^{(a)}\right] P_k(z,t) \tag{32}$$

In equations 31 and 32, ρ is the number density of active erbium atoms in the fiber core. The fiber has a cross section given by S and the excited state lifetime is τ. There are a total of N optical channels whose individual powers are $P_k(z,t)$. Γ_k is the confinement factor which indicates how much the transverse optical mode overlaps the uniform erbium distribution on the core of the fiber. $\sigma_k^{(e)}$ and $\sigma_k^{(a)}$ are the emission (e) and absorption (a) cross sections for the k^{th} channel. The variable u_k is a unit vector whose sign is positive for beams traveling from z = 0 to z = L and negative for beams traveling in the opposite direction. The power in the k^{th} channel P_k, has units of photons per unit time. Equation 32 can be solved for the upper state population N_2 and the result can be substituted into equation 31 to get

$$\tau u_k \frac{\partial}{\partial t}\left(\frac{1}{P_k}\frac{\partial P_k(z,t)}{\partial z}\right) = -u_k\left(\frac{1}{P_k}\frac{\partial P_k(z,t)}{\partial z}\right) - \frac{1}{P_k^{IS}}\sum_{j=1}^{N} u_j \frac{\partial P_j(z,t)}{\partial z} - \alpha_k \tag{33}$$

where $\alpha_k = \rho\Gamma_k\sigma_k^{(a)}$ is the absorption constant and $P_k^{IS} = S/\Gamma_k(\sigma_k^{(e)} + \sigma_k^{(a)})\tau$ is the intrinsic saturation power for the k^{th} channel. Integration from 0 to L with respect to z yields

$$\tau\frac{d}{dt}\left[\ln\frac{P_k^{out}(t)}{P_k^{in}(t)}\right] = -\ln\frac{P_k^{out}(t)}{P_k^{in}(t)} - \frac{1}{P_k^{IS}}\sum_{j=1}^{N}\left[P_j^{out}(t) - P_j^{in}(t)\right] - \alpha_k L \tag{34}$$

In equation 34, $P_k^{in}(t)$ and $P_k^{out}(t)$ represent the input and output powers of the k^{th} channel at time t. If we define $G_k(t) = ln[P_k^{out}(t)/P_k^{in}(t)]$ and $A_k = \alpha_k L$ then

equation 34 can be written as

$$P_k^{IS}\left[\tau\frac{dG_k(t)}{dt}+G_k(t)+A_k\right]=-\sum_{j=1}^{N}P_j^{in}(t)\left[\exp(G_j(t))-1\right] \tag{35}$$

Equation 35 can be solved numerically if initial conditions $P_k^{in}(t)$ and $G_k = G_k^0$ for all channels are known. The set of coupled ordinary differntial equations in 35 can be further reduced to a single equation. This is done by realizing that the right hand side of equation 35 is the same for all channels so that any two equations can be combined to obtain

$$\tau\frac{dG_{kj}(t)}{dt}+G_{kj}(t)+A_{kj}=0 \tag{36}$$

where $G_{kj} = P_k^{IS}G_k(t) - P_i^{IS}G_i(t)$ and $A_{kj} = P_k^{IS}A_k - P_i^{IS}A_i$. This first order differential equation can be solved to give

$$G_{kj}(t)=\left(G_{kj}^0+A_{kj}\right)\exp(\frac{-t}{\tau})-A_{kj} \tag{37}$$

where $G_{kj}^0 = P_k^{IS}G_k^0 - P_j^{IS}G_j^0$ is the given by the initial conditions. Now, the gain of the jth channel can be expressed in terms of the gain of the kth channel

$$P_j^{IS}G_j(t)=P_k^{IS}G_k(t)-\left(G_{kj}^0+A_{kj}\right)\exp\left(-\frac{t}{\tau}\right)+A_{kj} \tag{38}$$

Now the single decoupled ordinary differential equation is found by substituting equation 38 into equation 35

$$\tau\frac{d}{dt}P_k^{IS}G_k(t)+P_k^{IS}G_k(t)+P_k^{IS}A_k \;=$$

$$-\sum_{j=1}^{N}P_j^{in}(t)\left\{\left[\left(P_k^{IS}G_k(t)-(G_{kj}^0+A_{kj})\exp(-t/\tau)+A_{kj}\right)/P_j^{IS}\right]-1\right\} \tag{39}$$

The gain of the kth channel can be found using equation 39 and then substituted into equation 38 to find the gain in all of the other channels. In steady state at t = 0, $G_{kj}^0 + A_{kj} = 0$ in equations 38 and 39.

Numerical Simulations

The literature shows that the analytical solutions to the rate equations have been numerically simulated for a variety a system parameters. In [19], output power excursion is calulated for a WDM link with eight optical channels and a two stage EDFA. Figure 8 compares the simulated results to experimental results when 1, 4 and 7 channels are dropped. In this case, each input channel has an input power of

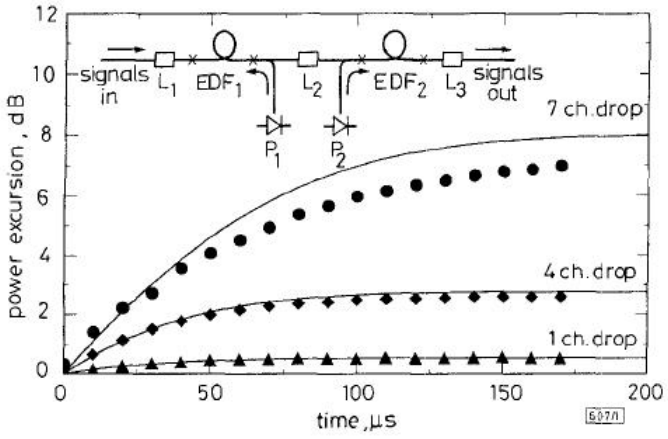

Figure 8: Comparison between theory an experiment for output power excursions of surviving channels from a two stage amplifier when 1, 4 and 7 channels are dropped [19]

-2 dBm and the gain of eah EDFA is 9 dB. The pump powers for the two stages are 18 dBm and 18.4 dBm for EDFAs 1 and 2 respectively. Reference [19] shows that transients can be large for systems with only two EDFAs.

A more detailed analysis is given by [7], where a cascade of 12 EDFAs with 8 WDM channels are simulated. In this case, the input channel power is -3 dBm and the pump powers are 19 dBm. The loss between each amplifier and the gain at each amplifier is equal to 10 dB. Figure 9 shows the signal power excursions as a function of time when 4 of the 8 channels are dropped. In figure 9, it is apparent that as the

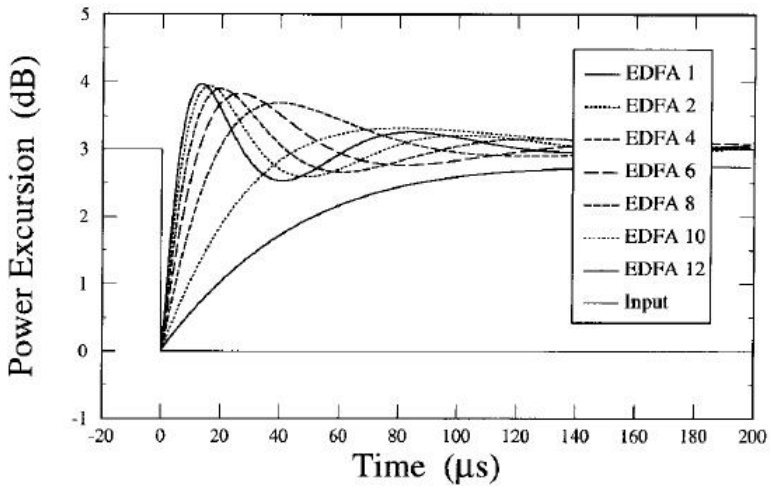

Figure 9: Total signal power excursions as a function of time from numerical simulation [7]

.

number of EDFAs in the chain increases, so does the peak power deviation and the frequency of oscillation.

In the previous two examples, the EDFAs did not have any internal gain control. There are several ways of controlling EDFA gain as discussed in the introduction and one of the most common methods is to use optical feedback in a ring configuration where a portion of the output optical power is fed back through to the input of the EDFA to clamp the gain. Several of the EDFAs used in the experiment described in chapter 4 employ this type of internal gain control so it is useful to examine the simulation presented in [24]. For this model, 16 channels with input powers of 10 μ W were used as steady state inputs. The pump source had a wavelength of 1480 nm and 200 mW of power. The time dependence of the output signals are shown in figure 10. Figure 10 shows that even systems with EDFAs that employ internal gain control can still produce large optical power excursions.

All the the models presented thus far simulate EDFA response to an abrupt change in input optical power. To simulate the effects of the power shaping technique, a

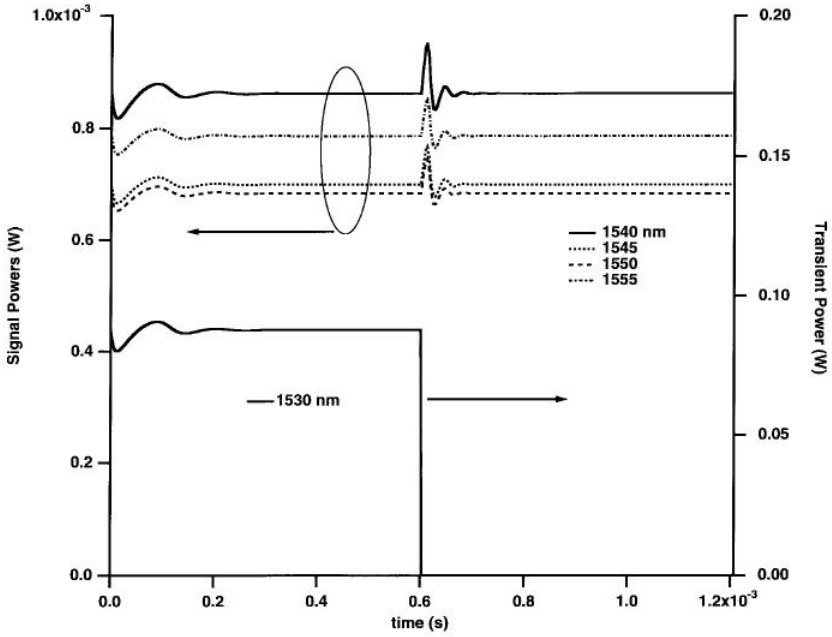

Figure 10: Time dependence of output signals (left axis) during a 1 x 10^{-4} W transient step of input signal at 1530 nm (output: right axis) [24].

model for a chain of 10 optically gain-clamped EDFAs where shaped heads and tails are added to signal bursts in order to gradually change the input optical power is discussed in [15]. A comparison of simulation results for optical power transients on a surviving channel with and without power shaping is shown in figure 11. The results from this analysis show good agreement with experimental results presented in chapter 4.

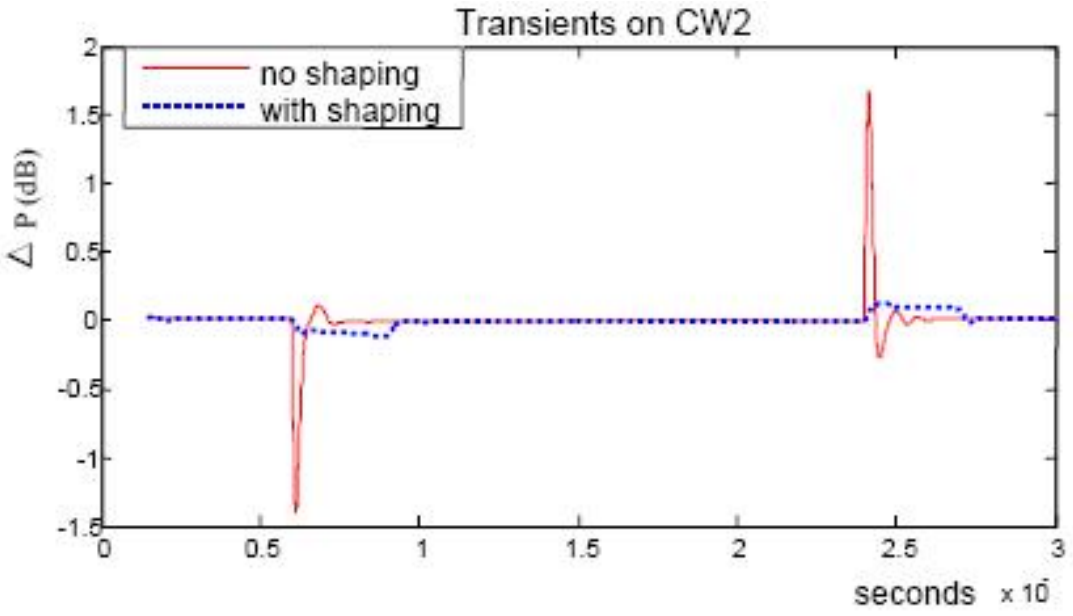

Figure 11: Comparison of power transients on channel 2 with and without power shaping [15].

OPTICAL TRANSIENT AMPLITUDE MEASUREMENTS

Introduction

This chapter presents the experimental setup and measurement techniques used for characterizing EDFA transients caused by data bursts in an optical network. Shaped heads and tails were affixed to data bursts in order to gradually change the optical power in the event of a rapid change in the optical power of the network. The focus of these experiments was to measure the effects of the gradual power change on the amplitude of optical power transients. In order to measure these effects, a long haul optical network was emulated in the laboratory using a chain of several EDFAs seperated by attenuators to emulate fiber loss. A programmable bit error rate test set (BERT) was used to modulate one laser transmitter with the desired data bursts while another continuous wave laser was used as a probe. Optical transient amlitude on the probe channel was measured for heads and tails of varying lengths on the modulated channel and an evaluation of the relationship between transient amplitude and the length of the shaped heads and tails, or shaping period, is presented.

Experimental Setup

The experimental setup used to suppress EDFA transients is shown in figure 12. A continuous wave probe laser at a wavelength of 1560.67 nm was coupled via a 3 dB coupler with the switching laser whose wavelength was set at 1554.14 nm. Both laser transmitters are shown in appendix B. The average output power of the switching laser was measured to be roughly 5 mW and could not be internally adjusted. The output power of the probe laser could be adjusted via internal gain control and was

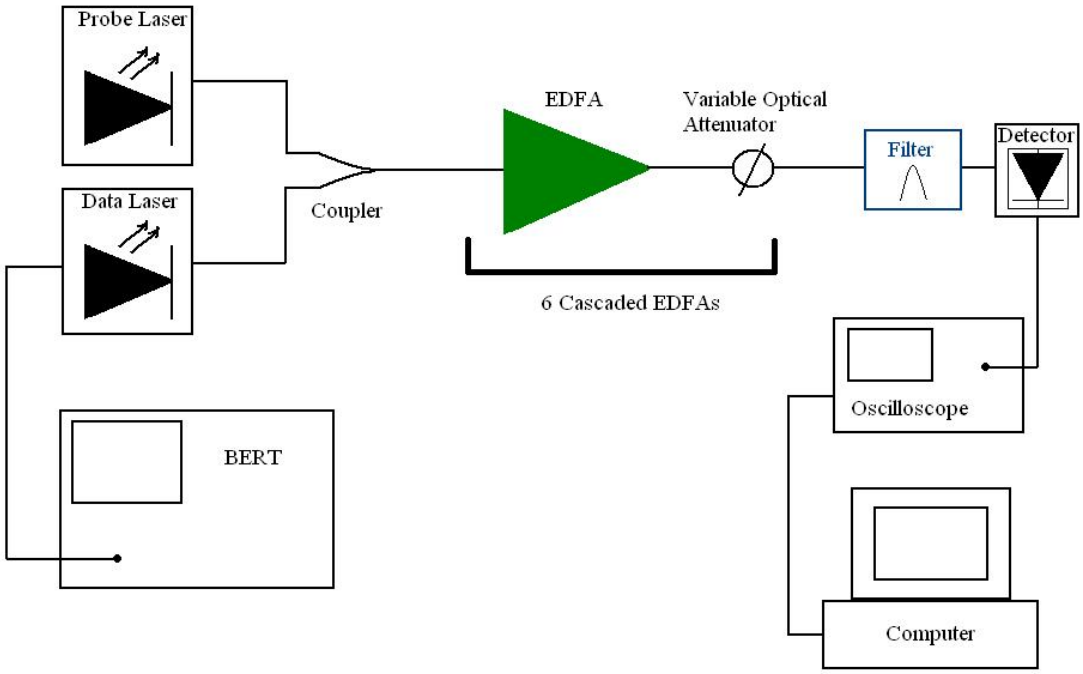

Figure 12: Experimental setup for testing the power shaping technique [25]

set to 5 mW to match the power level of the switching laser. Since it is common for each channel in a multi-wavelength network to operate with an optical power of about 1 mW, this experimental configuration is an emulation of an optical network with ten, 1 mW channels where 5 of the channels (the switching laser) would be added or dropped [25].

From the coupler, the laser signals are sent through a series of six EDFAs with attenuators between them to emulate a fiber span. Two types of optical attenuators were used to simulate fiber losses. The first type were voltage-controlled attenuators (VCAs) and were controlled via a USB connection to a computer running LabView software. The LabView control program for these attenuators allows the user to adjust and monitor the attenuator voltage and the corresponding optical attenuation

and is shown in appendix A. The second type of attenuators used for the experiment were blocking-type attenuators that could be manually adjusted. There was no reason for using the two different types of attenuators other than the fact that they were available for use and both are equally suited for this application.

Several different types of EDFAs were used in the experiment which was a result of availability and the fact that real optical networks might also employ several different types of amplifiers. Some of the amplifiers used in the experiment have internal gain control while others do not. Also, the different brands of amplifiers have slightly different gain specifications. The types of amplifiers used in the experiment are listed below and their individual specifications can be found in appendix B.

- 2 Bookham MGMFL-1AEC28
- 1 Bookham MGMFL-AWC28
- 2 JDS Uniphase OA 500
- 1 Jiasys ATE 101

Between each amplifier, the attenuators were used to adjust losses to match the gains such that each EDFA operated in saturation, which is the typical mode of operation for multi-wavelength optical networks. At the output of the amplifier chain, the probe laser light was filtered from the switching laser light using a waveguide demultiplexer with 50 GHz channel spacing, a flat top pass band profile, and adjacent crosstalk of -23 dB (appendix B). The probe laser light was then sent to a 1 GHz bandwidth detector whose output was connected to an oscilloscope. To record and measure the optical transients, a GPIB connection was used from the oscilloscope to a desktop computer running LabView software. The LabView program used to acquire the data from the oscilloscope simply captures the voltage waveform points that are

displayed on the oscilloscope screen at the time of the capture and saves them as a data file on the computer as shown in appendix A.

The switching laser was turned "on" and "off" by a bit error rate test set (BERT). "On" in this case refers to a period of time when the source laser transmits a random bit pattern at 1.25 Gb/sec and during "off" periods no light is transmitted. This type of scenario corresponds to burst or packet switched traffic where periods of data transmission may be preceded or followed by optical silence in that particular channel. The resulting pattern had a period of 24 ms with a 50% duty cycle so that random data bits would be transmitted for 12 ms and then the laser would be turned off for 12 ms. To measure transients without power shaping, the switching laser was modulated by bursts of data that were turned on and off abruptly where the rise and fall times of the modulator were several orders of magnitude shorter than the period of an EDFA transient oscillation.

To measure the effects of power shaping, heads and tails were placed on the beginning and at the end of the data bursts so that the average power of the modulated channels would be changed gradually. The slow change in average power is achieved by gradually increasing the probability of a "1" to 0.5 for heads and gradually decreasing the probability of a "1" from 0.5 to 0 for tails as illustrated by figure 13.

Figure 13 shows a data burst with a head at the beginning and a tail at the end. The thick line shows the probability distribution of 1's in the shaping profile. The computer algorithm used to create the shaping profiles was written by [26] and is shown in appendix B. The algorithm deterministically creates the pattern distribution by comparing the value of the integral of the shaping function at each point in the integral to the percentage of 1's in the pattern up to that point. If the value of the integral at a given point is .34 and the percentage of 1's in the pattern preceeding that point is .33 then a 1 is inserted. If the percentage of preceeding 1's exceeds the

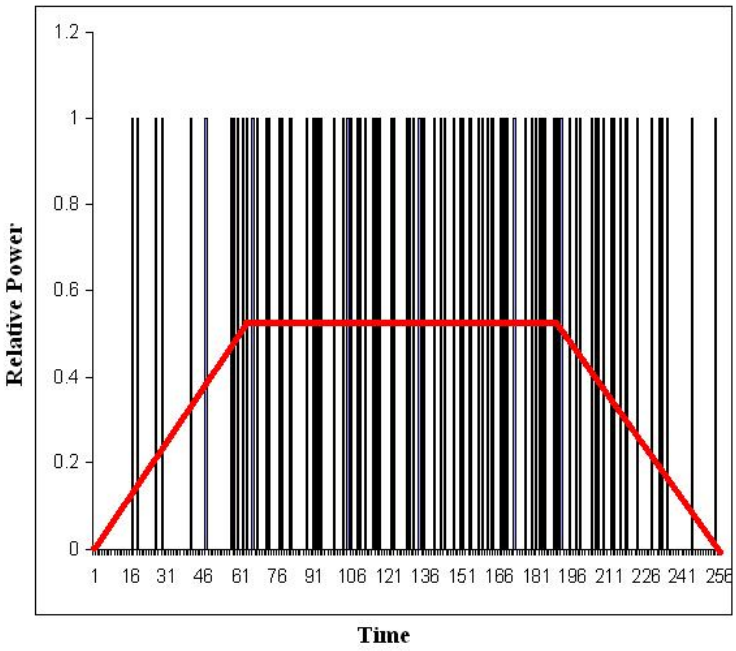

Figure 13: An illustration of how power shaping changes the average power at the beginning and end of a traffic burst. The thick line represents the average power of the data shown.

value of the integral then a 0 is inserted. For viewing purposes, the pattern shown in figure 13 is only 256 bits long which is much shorter than the actual shaping patterns used in the experiment and therefore does not appear to be a very good approximation of the probability distribution of the linear profile. The heads and tails of the actual patterns are a much better approximation to the probability distributions of the shaping profiles because there are many more bits within the profile yeilding a higher resolution in terms of average power distribution.

Transient Amplitude Results

The first set of experiments consisted of characterizing the transients produced by the EDFAs when no power shaping was applied. Figure 14 shows the induced

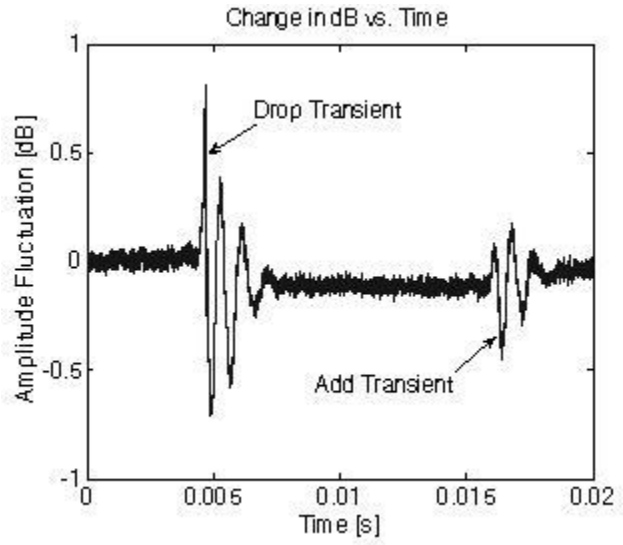

Figure 14: Measured transients for a chain of 5 EDFAs when no power shaping is applied [25]

transients on the probe channel when the switching laser transmitts data bursts with a period about 24 ms. Figure 14 shows two transients, the larger transient is where the switching laser was suddenly turned off (channel drop) while the smaller of the two transients is where the switching laser was turned on (channel add). The peak amplitude deviations of the drop and add transients are 0.85 dB and -0.45 dB respectively and the duration of the transients is on the order of 3 ms.

The amplitudes of the transients in figure 14 are plotted as the change in detector voltage relative to the steady state voltage, in dB, when both lasers are emitting light continuously. The detector is biased at 12.0 V so AC coupling was used on the input to the oscilloscope in order to measure the amplitude of the transients with high resolution in the voltage domain. To plot the transients in terms of delta dB, the deviation of the waveform must be compared to the steady state or DC level. This level was calculated using equation 40 after measuring the steady state optical power with an optical power meter.

$$V_o = P_o \Re(\lambda) R_{load} \tag{40}$$

In equation 40, V_o and P_o are the steady state voltage and optical power respectively, $\Re(\lambda)$ is the detector responsivity, and R_{load} is the value of the load resistor.

After measuring transients with no power shaping, heads and tails of various lengths were placed at the beginning and end of each traffic block. The shaping period, or time duration, of the heads and tails ranged from 500 μs to 4000 μs in increments of 500 μs. For each shaping period, four different shaping profiles were tested: linear, Gaussian, exponential and cosine squared. The four shaping profiles are defined by equations 41, 42, 43, 44, where t is time, A is the amplitude and τ is the full width at half-maximum.

$$P_{linear} = t \tag{41}$$

$$P_{Gaussian} = Aexp[-4\ln(2)(\frac{-t}{\tau})^2] \tag{42}$$

$$P_{exponential} = Aexp(t) \tag{43}$$

$$P_{cosinesquared} = A\cos^2(t) \tag{44}$$

The shaping profile defines the probability distribution of 1's during the shaping period. An illustration of the probability distribution for the profiles of the heads and tails are shown in figure 15. During the experiment, the lengths of the head and tail were equal in all cases.

Linear Shaping Profile

Figure 16 shows a comparison of shaping period versus channel add/drop transient mean, peak amplitudes and error bars for the linear shaping profile. To compute

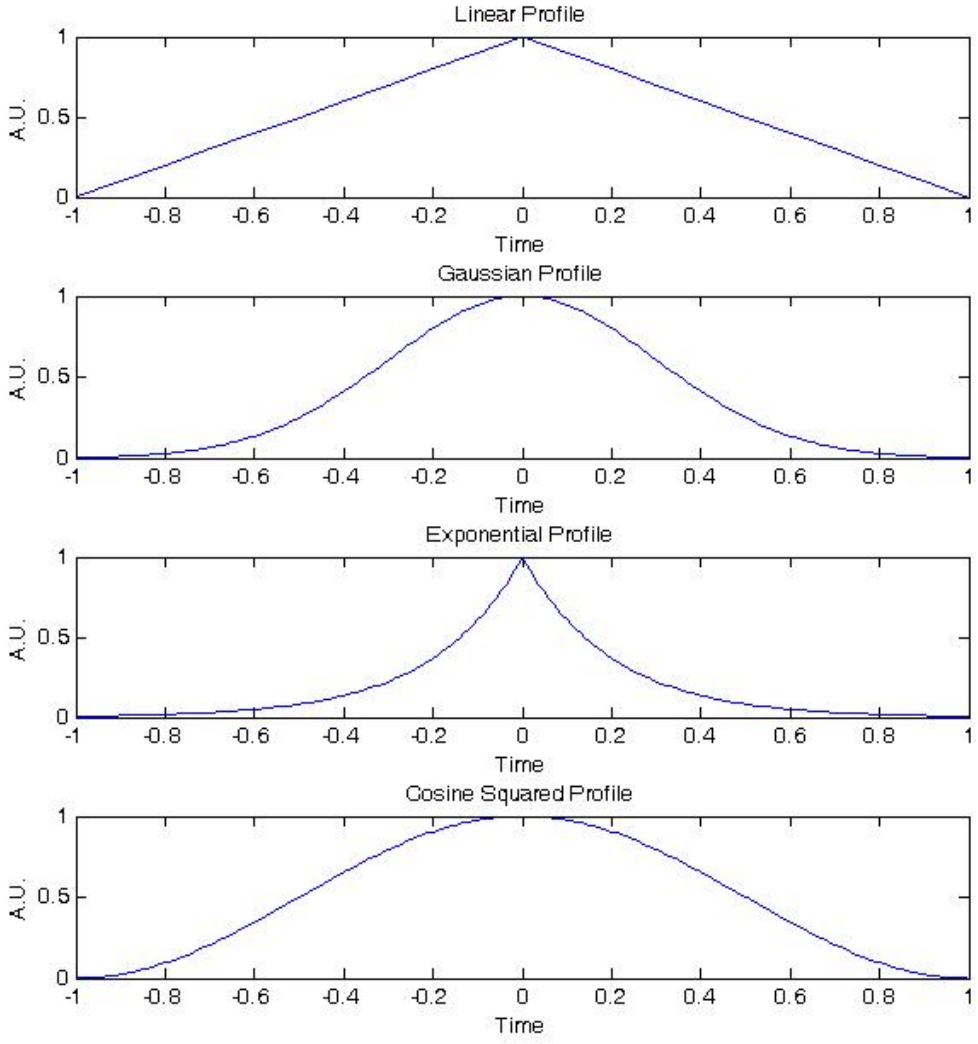

Figure 15: An illustration of of the probability distribution for each profile. The illustration shows only the head and tail of the pattern and not the data portion that would lie between the two shaping periods.

the mean and maximum values the add and drop transients needed to be seperated and analyzed individually. The duration of each transient oscillation was found by finding the point where the oscillation was roughly equal to the noise. After taking the absolute value of each transient, the mean was found by taking the mean of all the values within the duration of the transient. Similarly the maximum was found by taking the maximum of all of the values within the duration of the transient oscillation. The MATLAB program used to analyze the transient data for all of the shaping profiles is shown in appendix A. A series of ten consecutive measurements

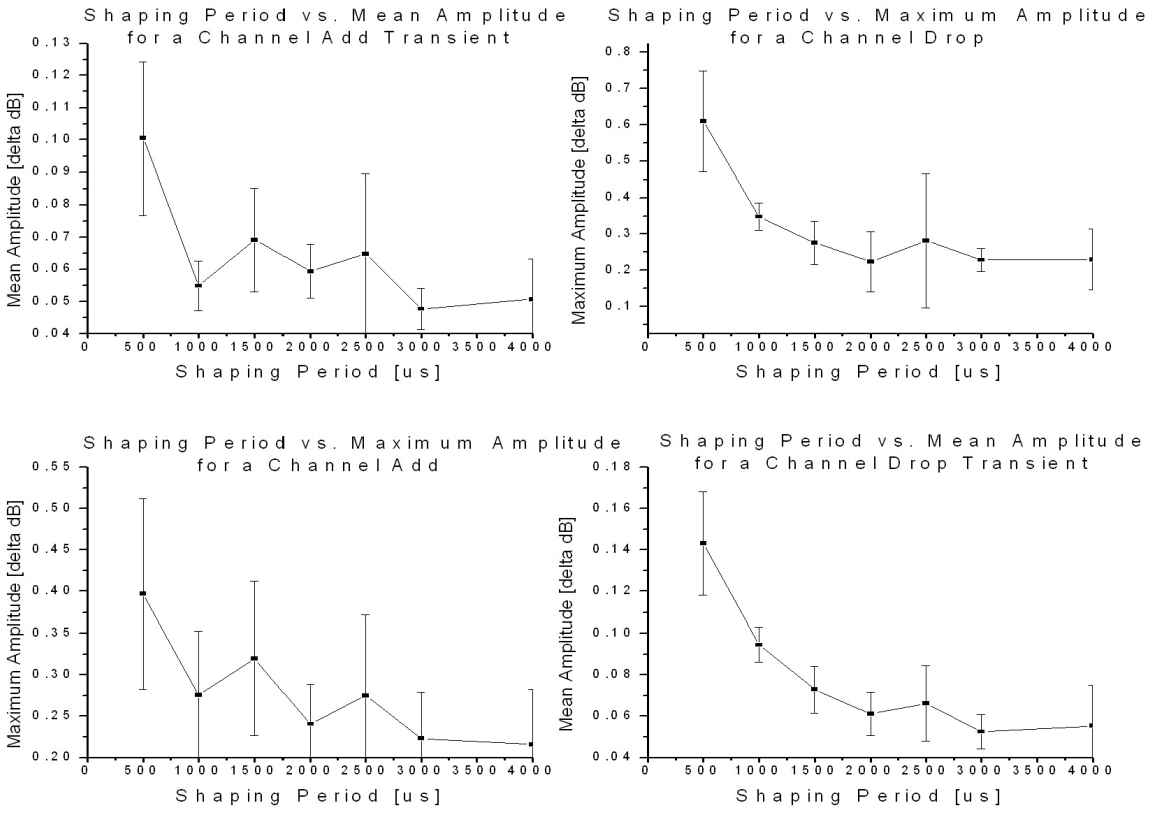

Figure 16: Transient maximum and mean amplitudes for the linear shaping profile.

were made for each data point in the plots shown in figure 16 in order to compute the error bars. The error bars shown here are the maximum errors in the measurements.

The error in the mean and maximum measurements of the add transients are generally larger than those shown for the drop transients. This is due to the fact that for our experimental setup, the add transients were smaller in amplitude than the drop transients so the signal to noise ratio was significantly lower. From figure 16, it is apparent that transient amplitude is reduced for both add and drop transients as the shaping period increases. The most pronounced effect is seen in the case of the maximum amplitude for a channel drop. In this case the transient amplitude drops from an amplitude deviation of about 0.62 dB down to 0.25 dB to give a reduction of about 0.37 dB. The mean amplitudes for add and drop transients are reduced by 0.06 dB and 0.09 dB respectively and the maximum amplitude of the add transient was reduced by 0.19 dB.

Gaussian Shaping Profile

After measuring the effects of the linear shaping profile, Gaussian shaped heads and tails were affixed to traffic bursts. These results are shown in figure 17. Figure 17 shows that while transient amplitude was reduced in most cases for the Gaussian profile, the effects were not as pronounced as with the linear profile. The greatest reduction in this case is seen in the maximum amplitude for a drop transient. In this scenario, the amplitude decreases from about 0.45 dB to roughly 0.25 dB for a reduction of about 0.2 dB. The maximum amplitude for a channel add stayed relatively constant in this case but the mean amplitudes for a channel add and a channel drop were reduced by 0.02 dB and 0.03 dB respectively.

An interesting feature of the plots for the Gaussian shaping profile is the pronounced hump at about 1500 μs which shows that the transients have greater amplitude at these shaping lengths than at shorter shaping periods. This is due to the fact that there are really two points during the shaping period that may cause an

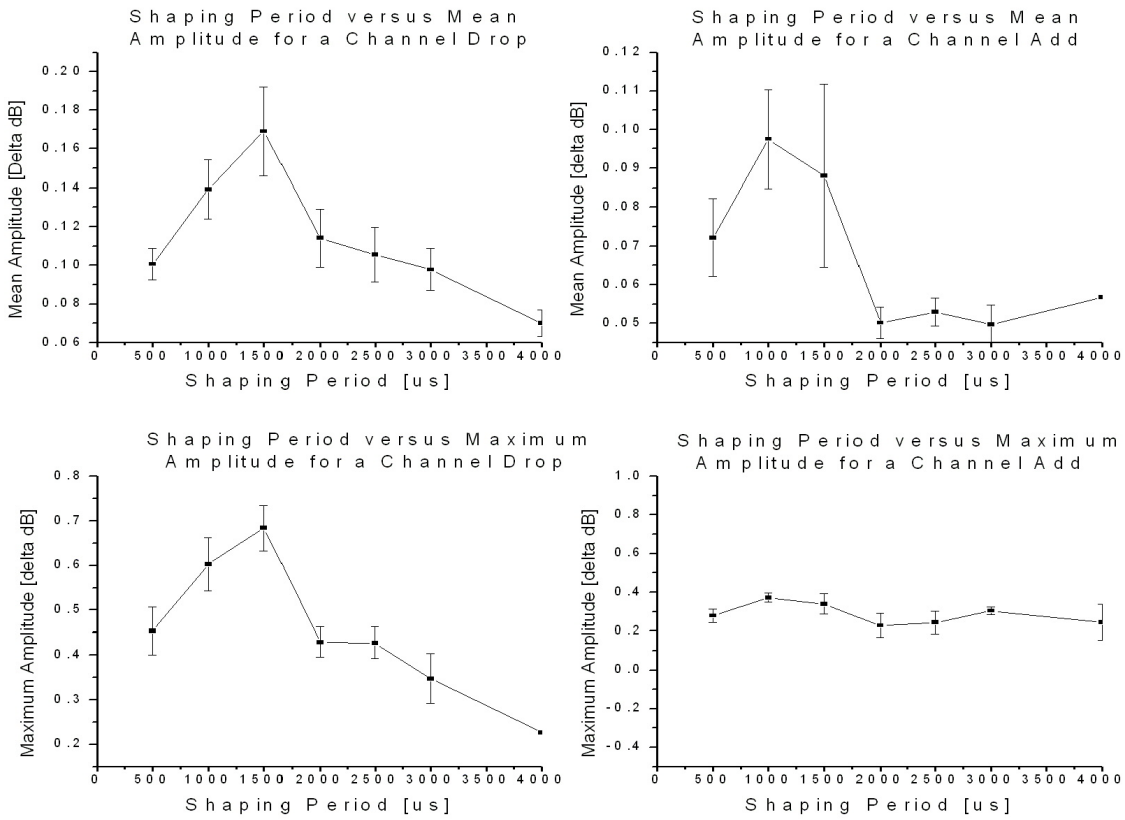

Figure 17: Transient maximum and mean amplitudes for the Gaussian shaping profile.

optical transient. The first point is located in the middle of the shaping pattern and the second point is at the beginning of the data portion at the end of the shaping pattern as illustrated by figure 18 and this effect is more pronounced with the Guassian shaping profile. The resulting transient is shown in figure 19.

By observing oscilloscope traces, the start of the transient was observed to be near the middle of the shaping pattern. For a 1500 μs pattern this means that the transient starts 750 μs after the beginning of the pattern and there is 750 μs until the end of the pattern and the start of the data portion. Also, the period of the transient oscillation was found to be roughly 750 μs. So in the case of a 1500 μs pattern, the transient created at the middle of the shaping period adds constructively

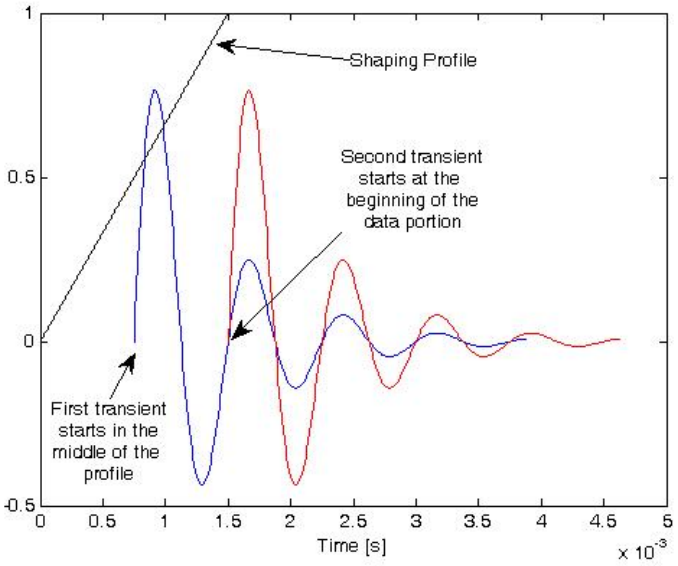

Figure 18: This picture illustrates how two transients are formed when the Gaussian shaping profile is used

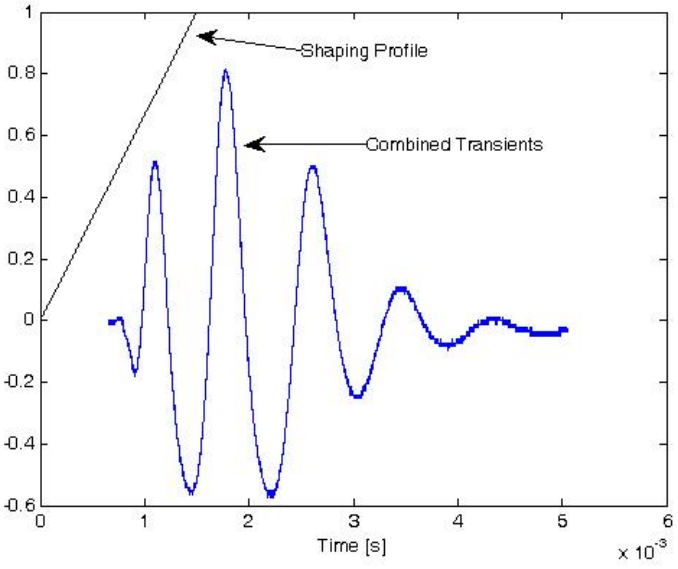

Figure 19: The combination of the two transients formed at the middle of the shaping profile and the beginning of the data portion.

to the transient created at the start of the data portion thus increasing the mean and maximum amplitudes of the transients.

Exponential Shaping Profile

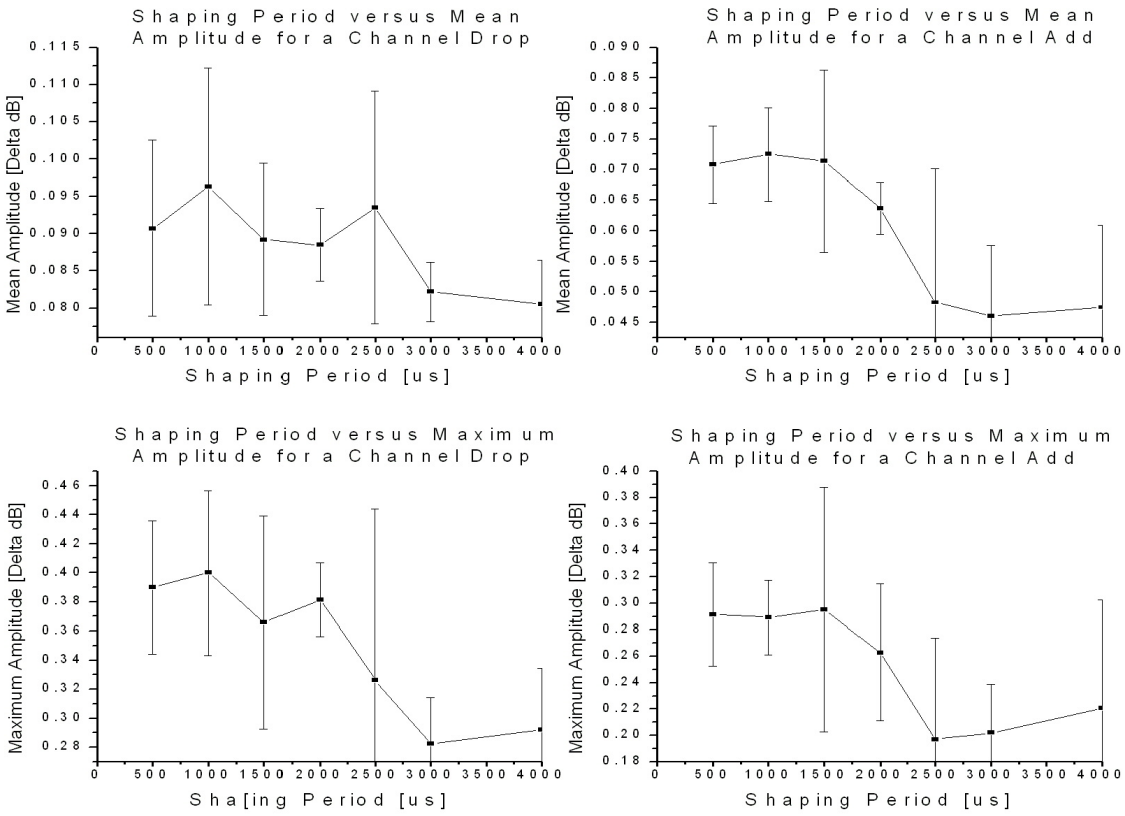

Figure 20: Transient maximum and mean amplitudes for the exponential shaping profile.

The results for transient amplitude versus shaping period for the exponential shaping profile are displayed in figure 20. As with the Gaussian shaping profile, there appears to be a hump in each plot that rolls off after 1500 μs. Since the exponential pattern is much steeper than the Guassian profile, the first transient starts closer to the end of the pattern instead of the middle. This means that constructive interference

between the transients at the two transitions happens at shorter shaping periods. This is why the hump starts earlier than those seen in the Gaussian profile. Figure 20 shows that the maximum transient amplitudes for a channel add and a channel drop are reduced by 0.1 dB and 0.11 dB. The mean amplitude of a channel add was reduced by about 0.03 dB and 0.01 dB for the drop transient.

Cosine Squared Shaping Profile

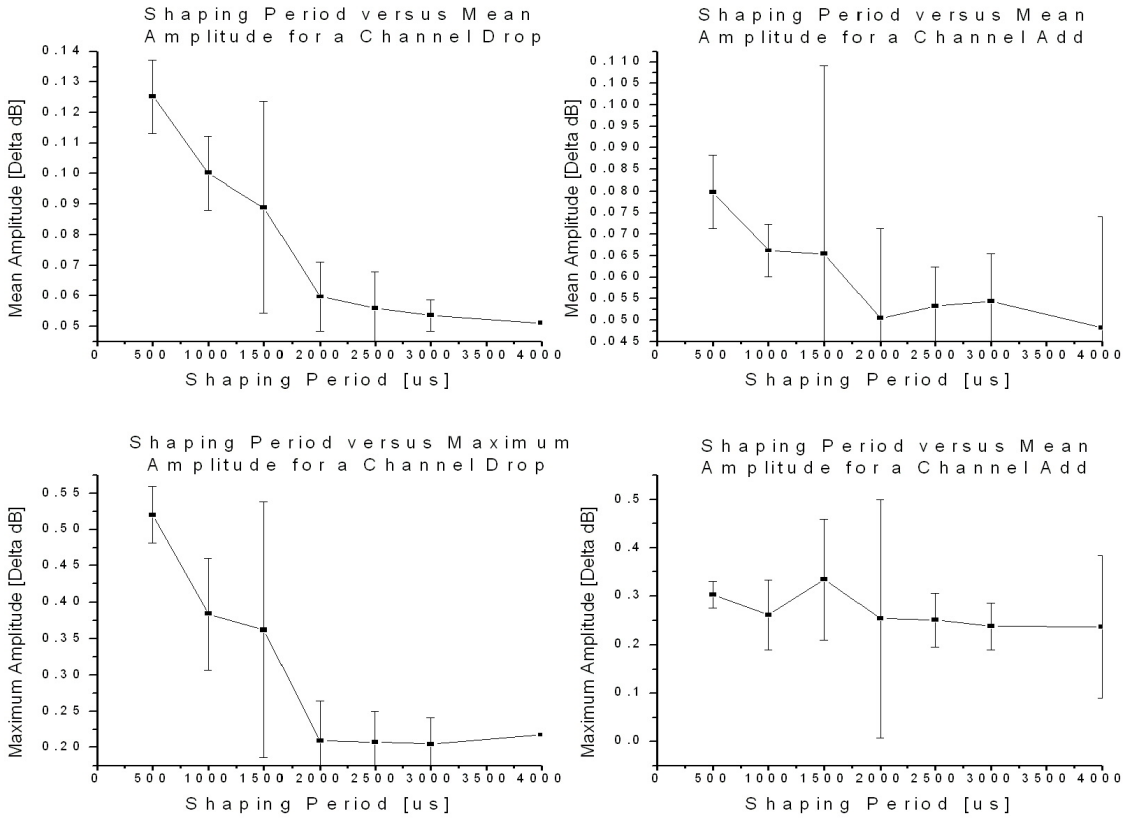

Figure 21: Transient maximum and mean amplitudes for the cosine squared shaping profile.

The results for the cosine squared shaping profile are plotted in figure 21. For the cosine squared profile, the maximum transient amplitude for a channel drop is reduced

from 0.52 dB down to 0.2 dB or 0.32 dB and the maximum of the add transient was reduced by about 0.05 dB. The mean amplitude for a drop transient in this case was reduced by 0.07 dB and 0.03 dB for an add transient.

Summary of shaping profiles

Each of the four shaping profiles have a unique effect on the the maximum and mean amplitudes of the switching transients. Figure 22 shows a side by side comparison of the four profiles. From figure 22 it is apparent that the linear and cosine

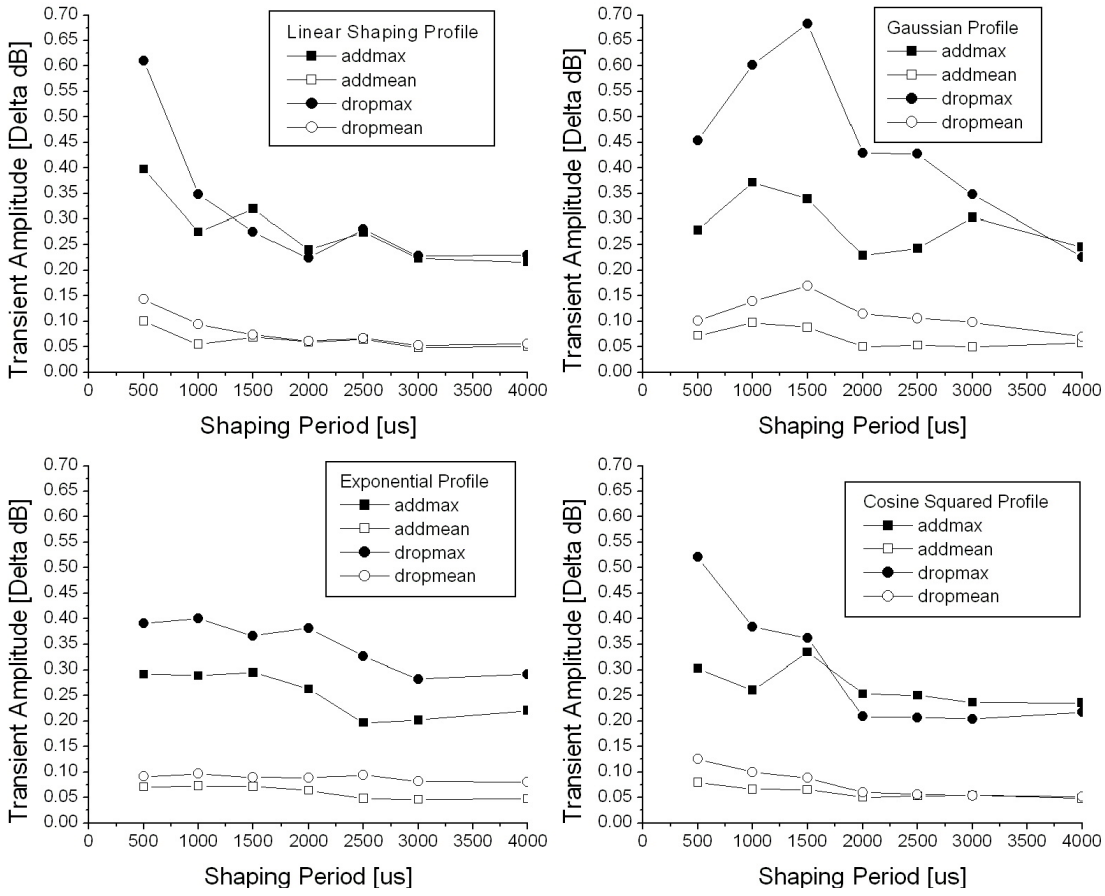

Figure 22: Comparison of the four different shaping profiles.

squared shaping profiles have the most pronounced effect on transient amplitude for both channel drop and channel add situations. However, it is interesting to note that

transient amplitude is initially lower for Gaussian and exponential shaping profiles even though the effect of longer shaping periods is less pronounced than in the linear profile case. Even though they are initially lower in amplitude, the linear and cosine squared profiles cause a greater reduction of the transient for shaping periods longer than about 2500 us. In terms of overall performance, it appears that a linear shaping profile performed the best in this scenario followed by the cosine squared profile. The exponential profile was not as effective as the cosine squared profile but performed slightly better than the Gaussian profile.

Figure 22 shows that optical amplifier transients can be significantly reduced for all shaping profiles with periods longer than about 3000 μs. In the case of the linear shaping profile, significant reduction occurs at a shaping period of about 1000 μs. The shaping periods needed to see a significant reduction in transient amplitude are relatively long in terms of modern optical network packet durations due to the use of high data rates. The relatively long shaping period is a result of the fact that the characteristic response time of the amplifiers is several milliseconds which is directly related to the excited state lifetimes for Erbium, as discussed in chapter 3. Also, the system ressponse time is a result of the number of EDFAs in the chain and whether or not the amplifiers have internal gain control mechanisims.

These experimental results compare favorably with simulations. In [15] the power shaping technique is modeled for chains of EDFAs and reduction in the amplitudes and durations of the transients associated with adding and dropping channels achieved by adding heads and tails to bursts are shown to be comparable.

BIT ERROR RATE MEASUREMENTS

Introduction

To characterize the power shaping technique in terms of network performance, an experiment was devised to measure the bit error rate (BER) of the probe channel as a function of the length of the heads and tails. To measure the BER of the probe laser, a bit error rate test set (BERT) was used to modulate the probe laser with a psuedo-random bit sequence (PRBS) and then measure the BER at the output. The BER was measured for all of the shaping periods of each shaping profile. The results show that the BER is reduced for increasing shaping periods for all shaping profiles.

Experimental Setup

In order to characterize the power shaping technique in terms of network performance, bit error rate measurements were made for the probe laser. These measurements were an investigation of the effects of switching transients on the integrity of the information being sent and received by the surviving channels. To make the bit error rate measurements, each laser was modulated with a separate bit error rate test set (BERT) as shown in figure 23.

The Agilent BERT was used to modulate the switching/data laser with the shaping patterns described in section 4. A second BERT (Anritsu) was connected to the internal modulator on the probe laser to meaure the BER on the probe channel. The bit rate on the Annritsu BERT could be adjusted from 1 Mbit/sec up to 700 Mbits/sec. For these tests, the Anritsu BERT was set to a bit rate of 600 Mbits/sec due to the fact that the internal modulator in the probe laser did not

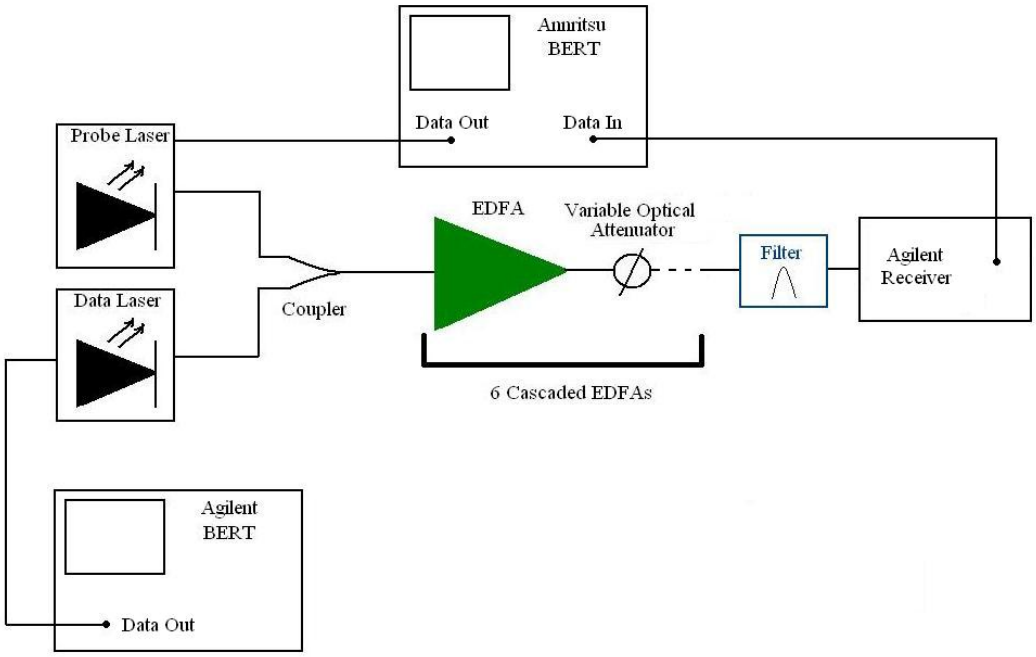

Figure 23: The experimental setup for measuring the bit error rate.

perform as well at other possible bit rates. Also, the pattern setting on the Annritsu BERT was set to a $2^{23} - 1$ psuedo-random bit sequence.

With sufficient power to the Agilent receiver, the probe channel was error free while the switching laser was being added or dropped. To create a measureable number of bit errors on the probe channel, the average power of the probe channel was reduced to the threshold of the receiver. At the threshold power of the receiver, the BER on the probe channel was roughly 3×10^{-6} or there were roughly 1800 bit errors per second. The burst period on the switching laser was 24 ms which gives approximately 42 bursts/sec. Also, the signal to noise ratio at the input to the receiver was measured to be 22 dB.

Bit Error Rate Results

To make the following measurements of the probe channel BER, the Anritsu BERT was set so that error counts were accumulated for thirty seconds. The final number of errors was then divided by thirty to get the average number of bit errors per second. The bit error rate for each profile is shown in figure 24.

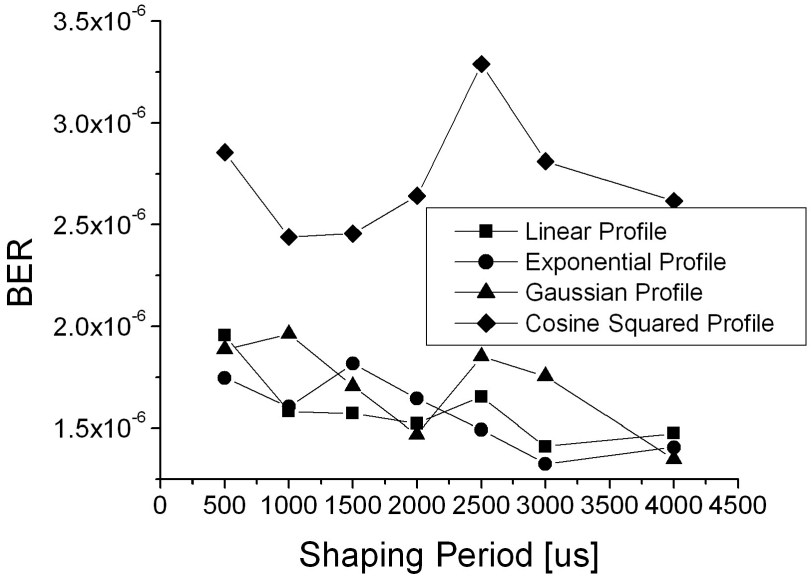

Figure 24: Summary of results for the BER experiments.

Figure 24 shows that the average BER is reduced for increased shaping periods. Each profile shows a fairly gradual reduction in the BER of 25% from about $1.8\times10^{-}6$ to about 1.4×10^{-6} with the exception of the cosine squared shaping profile. The cosine squared profile has a higher overall BER than the other three shaping profiles and does not exhibit the same gradual reduction in the BER for longer shaping periods. This behavior can be explained by considering the method in which the BER measurements are made. In order to create a measurable number of bit errors, the average power of the probe signal was reduced to the threshold of the detector. If

the DC optical power of the probe signal could be placed exactly at the threshold of the detector as shown in figure 25, then when transients were present, errors would occur when the probe power fell below the threshold and there would be no errors due to the transients when the probe signal power was above the detector threshold.

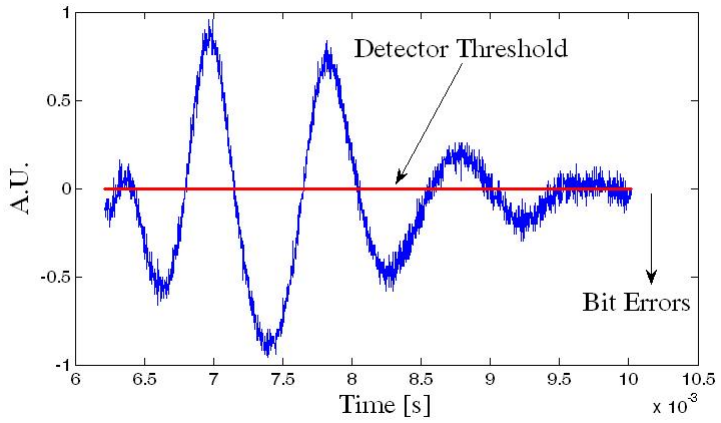

Figure 25: Illustration of the ideal scenario for the bit error rate measurements where the DC power level of the probe signal lies exactly at the threshold of the detector.

In this ideal scenario, bit errors would only be created by the low points in the transient oscillations. However, in practice, it is very difficult to adjust the power of the probe signal so that it lies exactly at the threshold of the detector. This is difficult because the threshold of the detetctor is not exactly known and because other factors such as temperature and the type of shaping profile may shift the DC optical power level of the probe signal. In the case of the cosine squared shaping profile, the DC optical power level of the probe signal was lower than the other shaping profiles and may have shifted below the threshold of the detector so that most or all of the transients waveforms were below the detector threshold as illustrated by figure 26. In this case, smaller transients would actually increase the BER because the lower amplitude causes the high points in the transient oscillations to fall even farther below

the detector threshold. If the DC power level of the probe signal could be adjusted more accurately, the BER rate measurements would be more conclusive.

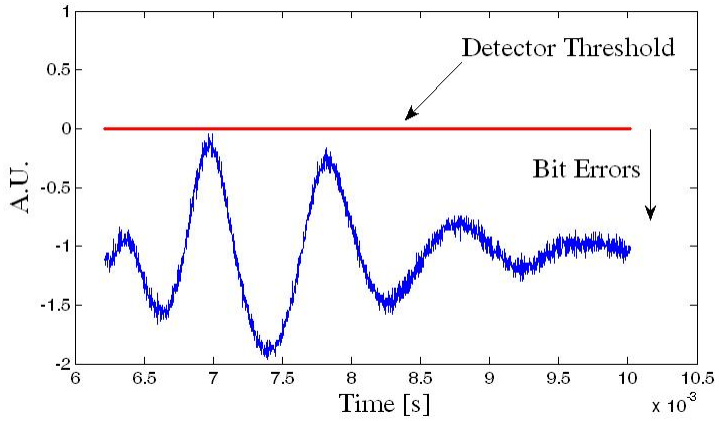

Figure 26: This figure shows how the transient oscillations may fall below the detector threshold.

CONCLUSION

EDFA transient effects can cause significant signal degradation in networks that dynamically add or drop channels, or where burst-type traffic is present. The amplitude of the transients is increased for increasing numbers of amplifiers in a chain. This thesis describes the theory of EDFA transients and the experimental investigation of a method of mitigating EDFA transients called power shaping where heads and tails are added to traffic blocks in order to gradually increase or decrease the average power on the channel. Laboratory experiments have shown the effectiveness of power shaping in terms of reduced transient amplitude and decresed bit error rates.

To measure transient amplitude for different shaping periods, four different shaping profiles were used: linear, exponential, cosine squared and Gaussian. Transient amplitude was measured for shaping periods from 500 μs to 4000 μs. All four of the shaping profiles caused a reduction in the amplitude of the switching transients but the linear profile caused the greatest overall reduction. The results presented in chapter 4 show good agreement with simulations described in [15].

The optimal choice for the head/tail duration depends on the characteristics of the system of interest. For the system described here, the optimal shaping pattern would be a linear profile with a 3000 μs shaping period. However, in some cases two transients are present and a cancelling effect could be achieved with proper shaping lengths depending on the response time of the entire system. System response time is dependent on the number of amplifiers in the chain and whether or not the EDFAs have internal gain control.

To characterize the power shaping technique in terms of network performance, bit error rate measurements were made. To measure the BER, the DC optical power was

reduced to the threshold of the detector so that power excursions would cause data loss. As the amplitude of the transients was decreased with longer shaping periods the BER was reduced. The linear, Gaussian and exponential profiles reduced the BER by similar amounts but the cosine squared profile had a higher overall BER. In this case it is believed that the DC optical power level was initially lower than the other profiles so that more bit errrors occurred. However, the BER was still reduced for the cosine squared profile for shaping periods greater than 3000 μs.

In contrast to other methods, power shaping does not require the addition of expensive and specialized electro-optic components or high power lasers. Power shaping could be implemented by adapting the existing link layer protocol. The power shaping concept could be applied to many other types of in-line amplifier technologies, although adjustment to shaping periods may be needed. Also, power shaping requires long shaping periods as compared to the bit duration in a modern communications network. For efficiency reasons the network designer may only want to attach shaping headers/trailers to long data bursts.

REFERENCES CITED

[1] R. Giles and E. Desurvire. Transient gain and cross talk in erbium-doped fiber amplifiers. *Opt. Lett. 14*, 16:880–882, 1989.

[2] K. Y. Ko et al. Transient analysis of erbium-doped fiber amplifiers. *IEEE Photon. Technol. Lett.*, 6(12):1436–1438, 1994.

[3] E. Desurvire. Analysis of transient gain saturation and recovery in erbium-doped fiber amplifiers. *IEEE Photon. Technol. Lett.*, 1(8):196–199, 1989.

[4] A. K. Srivastava et al. EDFA transient response to channel loss in wdm transmission system. *IEEE Photon. Technol. Lett.*, 9(3):386–388, 1997.

[5] L. Tancevski, A. Bononi, and L. A. Rusch. Output power and snr swings in cascades of edfas for circuit - and packet-switched optical networks. *IEEE J. Lightw. Technol.*, 19(7):933–940, 2001.

[6] M. Karasek, M. Menif, and L. A. Rusch. Output power excursions in a cascade of edfas fed by multi channel burst mode packet traffic: experimentation and modeling. *IEEE J. Lightw. Technol.*, 17(5):733–742, 1999.

[7] Y. Sun, J. L. Zyskind, and A. K. Srivastava. Average inversion level, modeling, and physics of erbium-doped fiber amplifiers. *IEEE J. Sel. Topics in Quantum Electronics*, 3(4), 1997.

[8] M. Karasek, A. Bononi, L. A. Rusch, and M. Menif. Gain stabilization in gain clamped edfa cascades fed by wdm burst-mode packet traffic. *J. of Lightw. Technol.*, 18(3):308–313, 2000.

[9] Okamura H. Automatic optical loss compensation with erbium-doped fiber amplifiers. *IEEE Lightwave Technol.*, 10:1110–1116, 1992.

[10] C. Tian and S. Kinoshita. Analysis and control of transient dynamics of edfa pumped by 1480- and 980-nm lasers. *J. of Lightw. Technol.*, 21(8):1728–1733, 2003.

[11] A. V. Tran, C. J. Chae, R. S. Tucker, and Y. J. Wen. Edfa transient control based on envelope detection for optical burst switched networks. *IEEE Photon. Lett.*, 17(1):226–228, 2005.

[12] T. Shiozaki, M. Fuse, and S. Morikura. A study of gain dynamics of erbium-doped fiber amplifiers for burst optical signals. *ECOC2002*, 3:1–2, 2002.

[13] H. Feng, E Patzak, and J. Saniter. Methods for stabilizing the gain of edfas in burst switching optical networks. *Photon. Net. Comm.*, 4(2):151–166, 2002.

[14] D. H. Richards, J. L. Jackel, and M. A. Ali. A theoretical investigation of dynamic all-optical automatic gain control in multichannel edfa's and edfa cascades. *IEEE J. Sel. Topics in Quantum Electronics*, 3(4), 1997.

[15] W. Lin, R. S. Wolff, and B. Mumey. Decreasing edfa transients by power shaping. *WOC'07*, 2007. Montreal, Canada.

[16] Reisfeld Renata and Christian K. Jorgensen. *Lasers and Excited States of Rare Earths*, pages 73–76. Springer–Verlag, 1977.

[17] Olsson N. A. Becker P. C. and Simpson J. R. *Erbium-Doped Fiber Amplifiers Fundamentals and Technology*, pages 133–139. Academic Press, 1999.

[18] B. Pedersen et. al. *J. Lightw. Technol.*, 9:1105, 2007.

[19] Y. Sun et. al. Model for gain dynamics in erbium-doped fiber amplifiers. *IEEE Elect. Lett.*, 32(16), 1996.

[20] Desurvire E. *Erbium-Doped Fiber Amplifiers.* John Wiley and Sons, New York, 1994.

[21] Morkel P. R. and Laming R. I. Theoretical modeling of erbium-doped fiber amplifiers with excited state absorption. *Opt. Lett.*, 14:1062–1064, 1989.

[22] Saleh A. A. M. et. al. Modeling of gain in erbium-doped fiber amplifiers. *IEEE Photonics Technol. Lett.*, 2:714–717, 1990.

[23] Jopson R. M. and Saleh A. A. M. Modeling of gain and noise in erbium doped fibre amplifiers. *SPIE fiber laser sources and Amplifiers III*, 1581:114–119, 1991.

[24] Chinn S. R. Simplified modeling of transients in gain-clamped erbium-doped fiber amplifiers. *Journ. of Lightwave Technol.*, 16(6):1095–1100, 1998.

[25] T. Jackson, M. Lee, Timothy Hahn, W. Lin, R. S. Wolff, and B. Mumey. Edfa transient reduction using power shaping. *WOC'08*, 2008. Quebec, Canada.

[26] Timothy Hahn and Brendan Mumey. Patterngenerator.cpp, 2008. Montana State University, Dept. of Computer Science.

APPENDICES

APPENDIX A

COMPUTER PROGRAMS

Transient Analysis Program

```
clear all
close all

% Trent Jackson
%   June 13, 2008
%   Description: Program takes user input path for location of data
%   and plots transient data. User specifies where to partition the data by
%   clicking on graph. Each partition is detrended and normalized by
%   detector response to plot in dB

% Select the operation
k = menu('Transient analysis program','Compute mean and max for one measurement',
'Compute mean and max with error bars for 10 measurements');
digits(6);
switch k
    case 1
        % load data and seperate amplitude and time data
        path = input('Please enter data path: ');
        sspower = input('What is the steady state optical power in watts?: ');
        responsivity = .95
        impedance = 50
        ssvoltage = sspower*responsivity*impedance;
        disp('Steady state voltage =');
        ssvoltage
        A = load(path);
        amplitude = A(:,1);
        t = A(:,2);

        % plot the original data
        figure(1)
        plot(t,amplitude),title('Plot of Voltage vs Time')
        xlabel('time (s)'),ylabel('Voltage (V)')

        % Get the start and stop location of each partition
        disp('Select begining and end location of first partition')
        [x1,y1] = ginput(2);
```

```
disp('Select␣begining␣and␣end␣location␣of␣second␣partition')
[x2,y2] = ginput(2);

% Check to see if points are valid
if x1(1) > x1(2) || x2(1) > x2(2)
    error('Points␣specified␣are␣not␣valid')
end
close(figure(1));

% locate indices near to where the user clicked
i1 = find(t > x1(1),1);
i2 = find(t > x1(2),1);
i3 = find(t > x2(1),1);
i4 = find(t > x2(2),1);

% partition at given indices
amppart1 = amplitude(i1:i2);
amppart2 = amplitude(i3:i4);
tpart1 = t(i1:i2);
tpart2 = t(i3:i4);

%Take the absolute value of the waveform and find the mean deviation
dt1 = detrend(amppart1);
dt2 = detrend(amppart2);

VdB1 = vpa(20*log(dt1 + ssvoltage));
VdB1_mean = vpa(mean(VdB1));
offset_VdB1 = vpa(VdB1 - VdB1_mean);
mean_dB1 = vpa(mean(abs(offset_VdB1)))

VdB2 = vpa(20*log(dt2 + ssvoltage));
VdB2_mean = vpa(mean(VdB2));
offset_VdB2 = vpa(VdB2 - VdB2_mean);
mean_dB2 = vpa(mean(abs(offset_VdB2)))

%Find the maximum
max_dB1 = vpa(max(abs(offset_VdB1)))
max_dB2 = vpa(max(abs(offset_VdB2)))
```

```
    %Plot the transients in delta dB
    plot(tpart1,offset_VdB1)
    xlabel('Time [s]')
    ylabel('Transient Amplitude [delta dB]')
    title('Transient Amplitude vs. Time')

    figure(2)
    plot(tpart2,offset_VdB2)
    xlabel('Time [s]')
    ylabel('Transient Amplitude [delta dB]')
    title('Transient Amplitude vs. Time')

case 2

    sspower = input('What is the steady state optical power in watts?: ');
    responsivity = .95
    impedance = 50
    ssvoltage = vpa(sspower*responsivity*impedance);
    ssvoltage

    data_mean1 = ones(1,7);
    data_mean2 = ones(1,7);
    data_mean_error1 = ones(1,7);
    data_mean_error2 = ones(1,7);
    data_max1 = ones(1,7);
    data_max2 = ones(1,7);
    data_max_error1 = ones(1,7);
    data_max_error2 = ones(1,7);

    for k = 1:7

        mean_dB1_1 = ones(1,10);
        mean_db2_1 = ones(1,10);
        max_dB1_1 = ones(1,10);
        max_dB2_1 = ones(1,10);

        for i = 1:10
            try
                path = input('Please enter data path: ');
```

```
        A = load(path);
    catch ME1
        ME1
        display('Please␣make␣sure␣there␣are␣single␣quotes
␣␣␣␣␣␣␣␣␣␣␣␣␣␣␣␣␣␣␣␣␣␣␣␣around␣the␣file␣path␣input␣and␣that␣the␣file␣name␣is␣correct')
        try
            path = input('Please␣enter␣data␣path:␣');
            A = load(path);
        catch ME2
            rethrow(ME2)
        end
    end

    amplitude = A(:,1);
    t = A(:,2);

    % plot the original data
    figure(1)
    plot(t,amplitude),title('Plot␣of␣Voltage␣vs␣Time')
    xlabel('time␣(s)'),ylabel('Voltage␣(V)')

    % Get the start and stop location of each partition
    disp('Select␣begining␣and␣end␣location␣of␣first␣partition')
    [x1,y1] = ginput(2);
    disp('Select␣begining␣and␣end␣location␣of␣second␣partition')
    [x2,y2] = ginput(2);

    % Check to see if points are valid
    if x1(1) > x1(2) || x2(1) > x2(2)
        error('Points␣specified␣are␣not␣valid')
    end
    close(figure(1));

    % locate indices near to where the user clicked
    i1 = find(t > x1(1),1);
    i2 = find(t > x1(2),1);
    i3 = find(t > x2(1),1);
    i4 = find(t > x2(2),1);
```

```
        % partition at given indices
        amppart1 = amplitude(i1:i2);
        amppart2 = amplitude(i3:i4);
        tpart1 = t(i1:i2);
        tpart2 = t(i3:i4);

        %Take the absolute value of the waveform and find the mean deviation
        dt1 = detrend(amppart1);
        dt2 = detrend(amppart2);

        VdB1 = vpa(20*log(dt1 + ssvoltage));
        VdB1_mean = vpa(mean(VdB1));
        offset_VdB1 = vpa(VdB1 - VdB1_mean);
        mean_dB1 = vpa(mean(abs(offset_VdB1)))

        VdB2 = vpa(20*log(dt2 + ssvoltage));
        VdB2_mean = vpa(mean(VdB2));
        offset_VdB2 = vpa(VdB2 - VdB2_mean);
        mean_dB2 = vpa(mean(abs(offset_VdB2)))

        %Find the maximum
        max_dB1 = vpa(max(abs(offset_VdB1)))
        max_dB2 = vpa(max(abs(offset_VdB2)))

        mean_dB1_1(i) = mean_dB1;
        mean_dB2_1(i) = mean_dB2;
        max_dB1_1(i) = max_dB1;
        max_dB2_1(i) = max_dB2;

        i = i + 1
    end

data_mean1(k) = vpa(mean(mean_dB1_1));
data_mean2(k) = vpa(mean(mean_dB2_1));
data_mean_error1(k) = vpa(abs(max(mean_dB1_1) - (data_mean1(k))));
data_mean_error2(k) = vpa(abs(max(mean_dB2_1) - (data_mean2(k))));
data_max1(k) = vpa(mean(max_dB1_1));
data_max2(k) = vpa(mean(max_dB2_1));
data_max_error1(k) = vpa(abs(max(max_dB1_1) - (data_max1(k))));
```

```
        data_max_error2(k) = vpa(abs(max(max_dB2_1) - (data_max2(k))));

        k = k + 1

        disp('Select the files for the next shaping length')
        end

        data_mean1
        data_mean2
        data_mean_error1
        data_mean_error2
        data_max1
        data_max2
        data_max_error1
        data_max_error2
end
```

Pattern Generator Program

```
// Timothy Hahn
// April 7, 2007
// Pattern Generator for BERT
// Reference: Decreasing EDFA Transients by Power Shaping
// Wenhao Lin, Richard Wolf, Brendan Mumey

#include<cstdlib>
#include<fstream>
#include<iostream>
#include<math.h>
#include<cmath>

using std::cin;
using std::cout;
using std::endl;
using std::flush;
using std::hex;
using std::ofstream;
using std::string;
```

```
enum function
{
  UNKNOWN,
  LINEAR,
  GAUSSIAN,
  COSINE_SQUARED,
  EXPONENTIAL
};

void getUserInput();
void openFile();
void writeFile();
void closeFile();
void generateSequence();
double cumulDist(double x, bool isHead);
void outputByte(unsigned char byte);

ofstream outputFile;

std::string headStr;

const double PI = 3.14159265358979323846264338327950288419764939937 5;

long int header_length;
long int data_length;
long int trailer_length;
long int zeros_length;
long int bitrate;
bool binaryOutput;

function function_type;

int main()
{
  getUserInput();
  openFile();
  writeFile();
  closeFile();
```

```
  return 0;
}

void getUserInput()
{
  char bora;

  cout << "IMPORTANT: Please enter integer numbers only!" << endl;

  cout << "How long would you like the header (in microseconds)? ";
  cin >> header_length;
  cout << "How long would you like the data (in microseconds)? ";
  cin >> data_length;
  cout << "How long would you like the trailer (in microseconds)? ";
  cin >> trailer_length;
  cout << "How long would you like the zeros (in microseconds)? ";
  cin >> zeros_length;
  cout << "What bit rate would you like (in Mbps)? ";
  cin >> bitrate;
  cout << "Would you like binary or ascii output (b or a)? ";
  cin >> bora;

  while(bora != 'b' && bora != 'B' && bora != 'a' && bora != 'A')
  {
    cout << "Would you like binary or ascii output (b or a)? ";
    cin >> bora;
  }

  if(bora == 'b' || bora == 'B')
  {
    binaryOutput = true;
  }
  else if(bora == 'a' || bora == 'A')
  {
    binaryOutput = false;
  }

  long int tmpFunction = 0;
```

```
while(tmpFunction <= 0 || tmpFunction > 4)
  {
    cout << "What function do you want 1:Linear, 2:Gaussian,
                3:Cosine Squared, 4:Exponential? ";
    cin >> tmpFunction;
  }

function_type = static_cast<function>(tmpFunction);

if(header_length % 16 != 0 && header_length > 0)
  header_length += 16 - (header_length % 16);

if(trailer_length % 16 != 0 && trailer_length > 0)
  trailer_length += 16 - (trailer_length % 16);

if(data_length % 16 != 0 && data_length > 0)
  data_length += 16 - (data_length % 16);

if(zeros_length % 16 != 0 && zeros_length > 0)
  zeros_length += 16 - (zeros_length % 16);

char temp[255];

sprintf(temp,"%d",header_length);
headStr = temp;
headStr.append("_");

sprintf(temp,"%d",data_length);
headStr.append(temp);
headStr.append("_");

sprintf(temp,"%d",trailer_length);
headStr.append(temp);
headStr.append("_");

sprintf(temp,"%d",zeros_length);
headStr.append(temp);
headStr.append("_");
```

```
  if(function_type == LINEAR)
    sprintf(temp,"Linear");
  else if(function_type == GAUSSIAN)
    sprintf(temp,"Gaussian");
  else if(function_type == COSINE_SQUARED)
    sprintf(temp,"CosineSquared");
  else if(function_type == EXPONENTIAL)
    sprintf(temp,"Exponential");

  headStr.append(temp);
  headStr.append(".ptrn");
}

void openFile()
{
  cout << "Opening files..." << flush;
  outputFile.open(headStr.c_str());
  cout << "done." << endl;
}

void writeFile()
{
  char funct[25];

  if(function_type == LINEAR)
    sprintf(funct,"Linear");
  else if(function_type == GAUSSIAN)
    sprintf(funct,"Gaussian");
  else if(function_type == COSINE_SQUARED)
    sprintf(funct,"CosineSquared");
  else if(function_type == EXPONENTIAL)
    sprintf(funct,"Exponential");

  outputFile << "Version=EPA 2.0" << endl;
  if(binaryOutput == true)
    outputFile << "Format=Bin" << endl;
  else
    outputFile << "Format=Ascii" << endl;
  outputFile << "Description=Power Shaping with Header = " << header_length
```

```
            << ", Trailer = " << trailer_length << ", Data = " << data_length
            << ", Zeros = " << zeros_length << ", Bit Rate of " << bitrate
            << ", and Function type of " << funct << endl;
  outputFile << "Count=1" << endl;
  //Seconds are in microseconds, so need to divide by 1,000,000 to
  //convert from seconds
  //Bitrate is in Mbps, so need to multiply by 1,000,000 to convert to bits
  //So just need to multiply by 1 to do both, i.e. 1,000,000 / 1,000,000 = 1
  outputFile << "Length=" << (header_length + data_length +
          trailer_length+zeros_length) * bitrate * 1 << endl;

  outputFile << "Data=" << endl;
  generateSequence();
}

void closeFile()
{
  cout << "Closing files..." << flush;
  outputFile.close();
  cout << "done." << endl;
}

double cumulDist(double x, bool isHead)
{
    if(function_type == LINEAR)
    {
      //cout << "returning " << 0.25 * pow(x,2) << endl;
      return(0.25 * pow(x,2));
    }
    else if(function_type == GAUSSIAN)
    {
      //TODO
      double sqrlog = sqrt(log(2.0));
      double valatzero = (0.0625 * ((sqrt(PI) * erf(4.0 * sqrlog * 0.0 -
                  4.0 * sqrlog)) / sqrlog));
      //cout << "returning " << (0.0625 * ((sqrt(PI) * erf(4.0 *
          //sqrlog * x - 4.0 * sqrlog))
          //cout / sqrlog)) - valatzero << endl;
      return(0.0625 * ((sqrt(PI) * erf(4.0 * sqrlog * x - 4.0
```

```
                * sqrlog)) / sqrlog)) - valatzero;
    }
    else if(function_type == COSINE_SQUARED)
    {
      //cout << "returning " << (( -0.50 * cos((PI * x)/2.0) *
                //sin((PI * x)/2.0) + 0.25
          //cout * x * PI)/PI) << endl;
      return(( -0.50 * cos((PI * x)/2.0) * sin((PI * x)/2.0) +
                0.25 * x * PI)/PI);
    }
    else if(function_type == EXPONENTIAL)
    {
      //cout << "returning " << (exp(5.0 * x - 5.0) / 10.0) << endl;
      return (exp(5.0 * x - 5.0) / 10.0);
    }

  return 0.0;
}

void generateSequence()
{
  if(header_length > 0)
    {
      cout << "Generating header..." << flush;

      long int numPoints = header_length * bitrate * 1;
      long int numOnes = 0;
      long int eight = 8;

      double curX, cumul;
      unsigned char byte;

      for(long int i = 0; i < numPoints; ++i)
      {
        curX = double(i) / double(numPoints-1.0);
        cumul = double(numOnes) / double(numPoints-1.0);

        short int mod = i - ((i / eight) * eight);
```

```
      if(cumul < cumulDist(curX,true))
      {
        byte |= unsigned(pow(2,8-mod-1));
        ++numOnes;
      }

      if(mod == 7)
      {
        outputByte(byte);
        byte = unsigned(0);
      }
    }
    cout << "done." << endl;
  }

if(data_length > 0)
  {
    cout << "Generating data..." << flush;
    for(long int d = 0; d < data_length * bitrate * 1; d = d + 8)
      {
        outputByte(char(170));
      }
    cout << "done." << endl;
  }

if(trailer_length > 0)
  {
    cout << "Generating trailer..." << flush;
    long int numPoints = trailer_length * bitrate * 1;
    long int numOnes = 0;
    long int eight = 8;

    double curX, cumul;
    unsigned char byte;

    unsigned char* trailer = new unsigned char[numPoints/8];

    for(long int i = 0; i < numPoints; ++i)
    {
```

```
        curX = double(i) / double(numPoints-1.0);
        cumul = double(numOnes) / double(numPoints-1.0);

        short int mod = i - ((i / eight) * eight);

        if(cumul < cumulDist(curX,true))
        {
          byte |= unsigned(pow(2,mod));
          ++numOnes;
        }

        if(mod == 7)
        {
          trailer[numPoints/8 - i/8 - 1] = byte;
          byte = unsigned(0);
        }
      }

      for(long int b = 0; b < numPoints/8; ++b)
      {
        outputByte(trailer[b]);
      }

      cout << "done." << endl;
    }

  if(zeros_length > 0)
    {
      cout << "Generating zeros..." << flush;
      for(long int z = 0; z < zeros_length * bitrate * 1; z = z + 8)
        {
          outputFile << (char)0;
        }
      cout << "done." << endl;
    }
}

void outputByte(unsigned char byte)
{
```

```
  if(binaryOutput == true)
  {
    outputFile << byte;
  }
  else
  {
    for(int i = 7; i >= 0; --i)
    {
      unsigned char powoftwo = unsigned(pow(2,i));
      if(unsigned(byte & powoftwo) > 0)
        outputFile << 1;
      else
        outputFile << 0;
    }

  }
}
```

LabView Programs

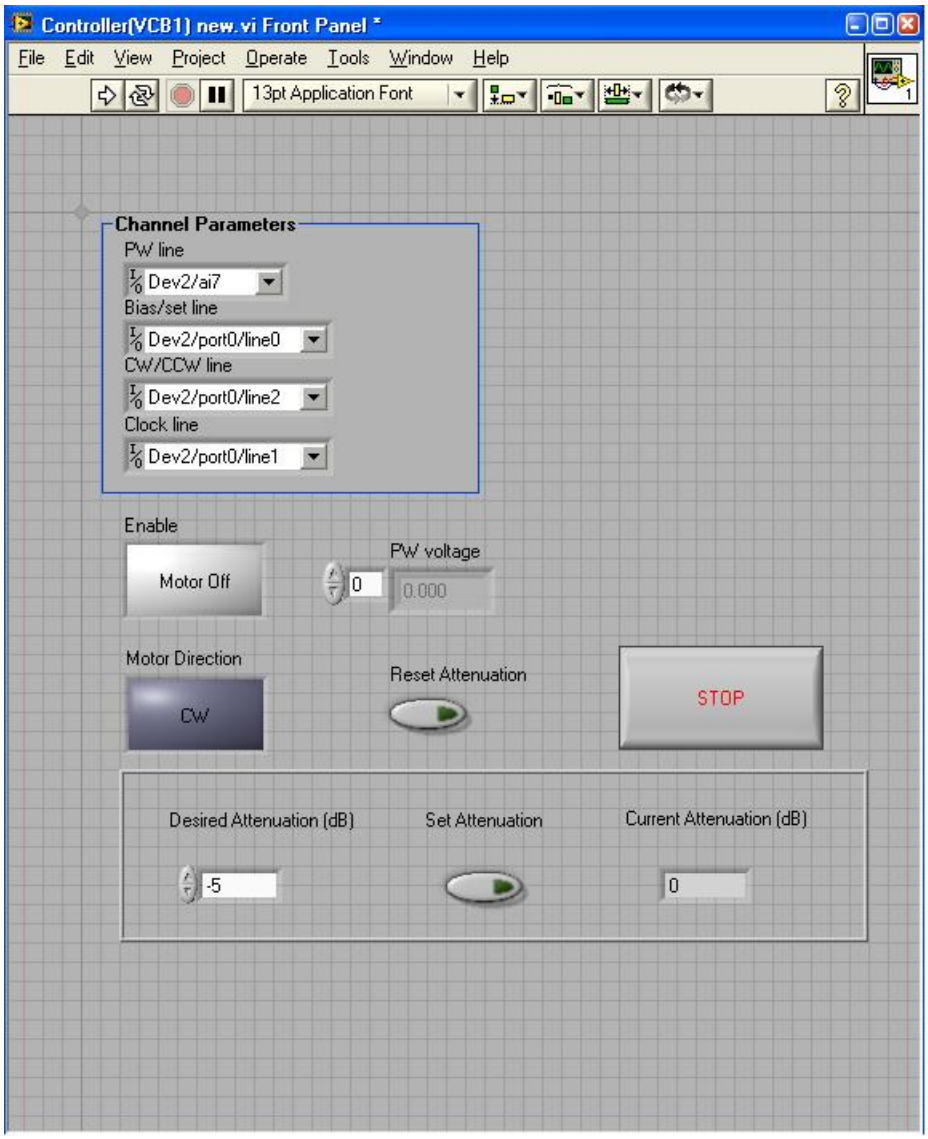

Figure 27: Labview Program Used to control the VCBs

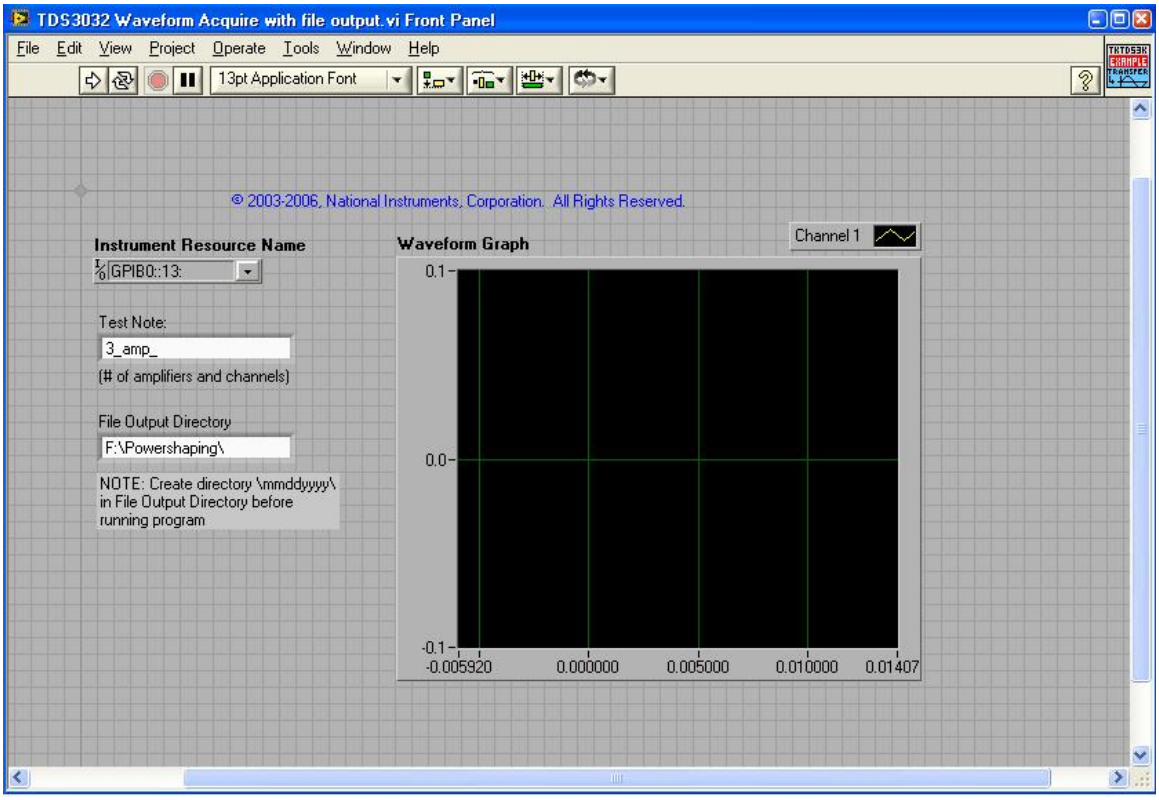

Figure 28: Labview program used to capture waveforms from the oscilloscope

APPENDIX B

LAB EQUIPMENT

Figure 29: Ortel laser bank

Figure 30: Agilent Transmitter

THORLABS INC PO Box 366, 435 Route 206N, Newton, NJ 07860
Ph (973) 579-7227, Fax (973) 300-3600, http://www.thorlabs.com

CE

D400FC InGaAs Fiber Optic Photo Detector

DESCRIPTION

Thorlabs DC400FC is a ready-to-use very high-speed photo detector. The unit comes complete with an FC/PC bulkhead connector / Detector and an internal 12V bias battery enclosed in a ruggedized insulated housing. A FC/PC type fiber optic bulkhead connector provides easy coupling to fiber based light sources. The output uses a SMA style jack for maximum frequency response.

SPECIFICATIONS

Detector:	InGaAs Pin	**Housing:**	Black Anodized Aluminum
Spectral Response:	800-1700nm	**Size:**	2.8" x 1.5" x 0.9"
Peak Response:	0.95 A/W @ 1550nm	**Bias:**	12V Battery (Type A23)
Rise/Fall Time:	0.1ns	**Output:**	SMA Plug
Diode Capacitance:	0.7pF (typ)	**Input*:**	FC/PC bulkhead fiber connector
NEP @ 1550nm:	1.0 x 10^{-15}W/√Hz	**Ball Lens Size:**	Ø0.058" (Ø1.47 mm)
Dark Current:	0.7nA (typ)	**Reflective Index of lens:**	1.482 @ 675nm
	1.0nA (max)	**Coupling Efficiency:**	92% (typ) into both single and multi-mode fibers over full spectral response of detector.
PD Active Diameter:	0.1 mm		
Bandwidth:	1GHz (min)	**Field of View (FOV):**	48°
Operating Temp:	0 to 40°C		
Storage Temp:	0 to 40°C		
Damage Threshold:	70 mW (max)		

* Note: The D400FC is not compatible with FC/APC fiber connectors.

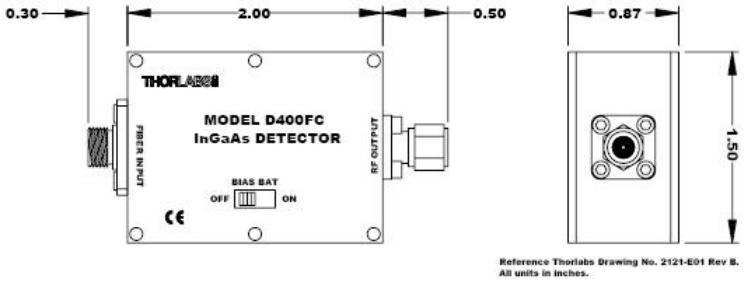

Figure 31: Thor Labs detector

Figure 32: Bookham EDFA

MGMFL-1AEC28 - Full Band Line Amplifier

Parameter	Min	Typ	Max	Unit	Notes
Operating wavelength	1530	1540	1563	nm	Calibrated to a of 1540 nm
Optical input power			-6	dBm	
Optical output power	17			dBm	-6 dBm input power, 1540 nm
Gain		23		dB	1540 nm, 40°C
Noise figure maximum			5.5	dB	Over wavelength range, -6 dBm I/P
Backward ASE			-25	dBm	
Remnant 980 to output			-30	dBm	
Remnant 1480 to input			-30	dBm	
Remnant 1480 to output			-30	dBm	
Gain flatness		1.0	1.5	dBpk-pk	23 dB gain 1540 nm, 17 dBm O/P, 40°C
PDG			0.5	dB	
PMD			1.0	ps	
Optical power monitor	1.0	2.5	5.0	%	
Optical input return loss			40	dB	Amplifier off
Optical output return loss			40	dB	Amplifier off
Gain control ripple			0.5	dB	15 dB Δ in input power
Power consumption		5	23.5	W	

Input port F
Output port E
Monitor port C

Figure 33: Bookham MGMFL-1AEC28

MGMFL-1AWC28 - Full Band Line Amplifier

Parameter	Min	Typ	Max	Unit	Notes
Operating wavelength	1530	1540	1563	nm	Calibrated to a λ of 1540 nm
Optical input power			-0.5	dBm	
Optical output power	17.5			dBm	-0.5 dBm input power, 1540 nm
Gain		18		dB	1540 nm, 40°C
Noise figure maximum		5.5	6.0	dB	Over wavelength range, -0.5 dBm I/P
Backward ASE			-25	dBm	
Remnant 980 to output			-30	dBm	
Remnant 1480 to input			-30	dBm	
Remnant 1480 to output			-30	dBm	
Gain flatness		1.0	1.5	dBpk-pk	18 dB gain 1540 nm, 17.5 dBm O/P, 40°C
PDG			0.5	dB	
PMD			1.0	ps	
Optical power monitor	1.0	2.5	5.0	%	
Optical input return loss			40	dB	Amplifier off
Optical output return loss			40	dB	Amplifier off
Gain control ripple			0.5	dB	15 dB Δ in input power
Power consumption		5	23.5	W	

Input port F
Output port E
Monitor port C

Figure 34: Bookham MGMFL-1AWC28

Figure 35: JDSU amplifier

Signal wavelength	1529 to 1562 nm
Total input signal power	-30 to 0 dBm
Total output signal power	15 dBm
Signal gain	24 dB
Noise figure	6.0 dB
Gain flatness	N/A
Dimensions (W x H x D)	70 x 90 x 12 mm
Operating temperature	0 to 70 °C
Power consumption	4.5 W

Figure 36: JDSU amplifier data

Thermally controlled AWG

NEL is the pioneer and market leader of AWG. NEL's AWG combines and splits optical signals of different wavelengths for use in WDM systems. The heart of the device, the AWG, consists of a number of arrayed channel waveguides that act together like a diffraction grating in a spectrometer.

FEATURE

* Low loss
* 25, 50, 100 and 200 GHz channel spacing
* Large channel number up to 128
* Polarization insensitive
* Highly stable and reliable
* Tested to Telcordia GR-1209 and GR-1221
* Module equipped with ATC (Automatic temperature controller) available
* MUX and DEMUX configuration available

APPLICATION

* Multi/demultiplexer for DWDM signal

	Gauss-type	Flat-type
Optical frequency	C- or L-band	
Channel spacing	100 GHz	
Channel number	40	
Insertion loss	< 3	< 5
Insertion loss Uniformity	< 1.5	
1 dB bandwidth	> 25	> 50
3 dB bandwidth	> 50	> 75
Polarization dependent loss	< 0.5 dB	
Adjacent crosstalk	< -23	
Total crosstalk	< -20	

Figure 37: AWG multi/demultiplexer used to filter the probe channel